A global climatology of the ocean surface during the Last Glacial Maximum mapped on a regular grid (GLOMAP) – Final response to referee comments

André Paul[1], Stefan Mulitza[1], Ruediger Stein[1, 2], and Martin Werner[2]

[1] MARUM – Center for Marine Environmental Sciences and Department of Geosciences, University of Bremen, Bremen, Germany

[2]Alfred Wegener Institute, Helmholtz Centre for Polar and Marine Research (AWI), Bremerhaven, Germany

Response to Anonymous Referee #1

We are thankful to the referee for the helpful and constructive comments that will surely improve our manuscript.

General comments

The authors state is that the Data-Interpolating Variational Analysis method is also capable of analyzing much sparser data. In the paper there is no real comparison or assessment of other methods that would allow the author to make this statement. So I would encourage the authors to add a few lines explaining their choice, maybe by adding some details on the methods that could justify their choice for the present study would be relevant and comparing with the methods employed to create CLIMAP and GLAMAP climatologies.

- In response to the valid concern raised by both referees, in the revised manuscript (p. 4, p. 6) we provide a test of the method by, as proposed by the second referee, withholding a certain fraction of the data, make a fit to the remaining data using DIVA, then compare the fit to the withheld data. We adopted the procedure by Schäfer-Neth et al. (2005), which allowed us compare our results to variogram analysis and kriging and the Levitus objective analysis.

- Furthermore, we took the opportunity to explain our choice of using DIVA (p. 4 of the revised manuscript) – for example, DIVA takes the coastlines into account, since an underlying variational principle is solved only on a finite-element mesh that covers the sea. This prevents the exchange of information across boundaries such as land bridges, peninsulas or islands, which might produce artificial mixing between, for example, Pacific and Atlantic water masses across the Panama isthmus. In solving the variational principle, it not only takes into account the distance between analysis and data, but also imposes a smoothness constraint and, if desired, an advection constraint, and moreover, it provides an uncertainty estimate.

- Regarding the method employed to create the CLIMAP climatology: As described in detail by Broccoli and Marciniak (1996; see also Manabe and Broccoli, 2020), CLIMAP used a subjective analysis procedure (i.e. contouring by hand) to

yield the paleoisotherm maps (CLIMAP Project Members, 1976, 1981), which were then digitized on a regular grid (see p. 2 of the revised manuscript).

- With respect to the GLAMAP climatology, different methods were applied: Contouring of the paleotemperature maps was also by hand, and the isotherms were derived by means of visual triangulation from strictly linear interpolation between the SST reconstructions at the irregularly distributed neighbor sites (Sarnthein et al., 2003; Pflaumann et al., 2003). For gridding, either the digitized isotherms (Paul and Schäfer-Neth, 2003) or the SST reconstructions at the sediment core positions (Schäfer-Neth and Paul, 2004) were objectively interpolated using variogram analysis and kriging in spherical coordinates; and the resulting gridded fields were compared (Schäfer-Neth and Paul, 2004, Fig. 5). The seasonal cycle was constructed in the same way as for the GLOMAP climatology: Following the PMIP (1993) guidelines, a sinusoidal cycle was fitted to the glacial-to-modern anomalies and then the modern monthly SST (taken as 10 m data from the WOA, 1998) was added.

- The variogram analysis and kriging cannot deal easily with coastlines, for example, it may take into account data points separated by a land bridge or an island. This was one motivation to apply the DIVA method (Troupin et al., 2012), which employs a finite-element mesh derived from a given topography.

Data availability: it would be useful for the reader to have the direct URL to avoid searching within the PANGEA database. I searched using "GLOMAP" as keyword (https://www.pangaea.de/?q=GLOMAP) but that request did not return any result, so I guess the data will be published once the paper is published. What is the format of the climatology?

Indeed, the final version of the data will be published in the PANGEA database once the paper is published. We already submitted our data to the PANGEA database. The format of the climatology is the Network Common Data Format (netCDF).

Some parts of the processing workflow (Section 2) were not totally clear to me, for example lines 89-109: why are the two steps necessary, and why not use all the data at the same time for the monthly interpolations?

We took two steps in order to make use of the diatom and radiolarian data from the Southern Ocean. Because in this region the biogenic particle flux to the sea floor is restricted to austral summer, even in areas unaffected by sea-ice cover (Abelmann and Gersonde, 1991; Gersonde and Zielinski, 2000; Fischer et al., 2002), only Southern Hemisphere summer (JFM) SST has been estimated by Gersonde et al. (2005). Therefore, in the first step, we only used the foraminiferal and dinoflagellate data for JAS and JFM. In the second step, we included the diatom and radiolarian data available for JFM and filled in the missing data for JAS by taking the results from the first step at the grid points where diatom and radiolaria data for JFM exist. In this way we were able to create monthly data at all grid points where data exist and repeat the DIVA analysis.

lines 94-94: To each sea-ice covered data point we assigned an error of 2°C $\longrightarrow$ does this mean that measurements taken where it is supposed to be sea ice are used for the gridding? From line 80, it seems that the finite-element mesh is based on a coastline from a glacial topography, so the measurements on ice would not influence the analysis.

Indeed, we used a glacial topography to generate the coastlines, however, these coastlines do not reflect the sea-ice edges (lines 104-105 of the revised manuscript). Therefore the finite-element mesh extended to the sea-ice covered regions. To utilze the information on past sea-ice coverage, we digitized the sea-ice edges, created monthly sea-ice masks and included the sea-

ice covered data points in the DIVA analysis. A relatively large error of 2 °C was assigned to each sea-ice covered data point to reflect the uncertainty in the LGM sea-ice extent reconstructions.

Could you add the figure of the coastline and the finite-element mesh in the Appendix?

We added maps of the coastlines and the finite-element meshes for both, the World Ocean Atlas (WOA) test of the DIVA method and the GLOMAP paleo-data analysis (Fig. A1).

Minor comments and typos

39: This method allows to take ⟶ allows one to take

Corrected (line 52 of the revised manuscript)

39: the uncertainty on the reconstruction ⟶ the authors probably means the uncertainties on the observations (instrumental errors, representativeness errors etc).

Indeed, we mean the paleo-data. Because these are not direct observations as instrumental data, but indirect estimates derived from fossil faunal assemblages using a transfer function technique, we often use the term "reconstruction", which may be confusing. Hence in the sentence in question we replaced "reconstruction" by "paleo-data" (line 53 of the revised manuscript).

40: or for assessing the data-analysis mismatch. ⟶ independently of the interpolation technique, the data-analysis mismatch is not always a relevant metrics: one can obtain a very small mismatch by forcing the analysis to be close to the observation. This would result in a "noisy" or "patchy" interpolated field, which may not represent what a climatology should be.

This is certainly true, thank you for pointing this out. Figures 3 and 4 show that the interpolated fields are neither "noisy" or "patchy", something that we now mention in the discussion of our results (lines 246–248 of the revised manuscript).

line 49: "we digitized sea-ice edges" ⟶ can you explicit what is the process to digitize? For Xiao et al. (2015, Fig. 7a), the panel a of their figure did not display any coordinates, how was that solved? Does this also means that no other publication provides the sea-ice edges in digital format?

It is indeed true that none of the publications provides the sea-ice edges in digital format. Therefore we had to digitize the curves from the published maps to obtain their location in geographic coordinates. In case of Xiao et al. (2015, Fig. 7a), neither the projection nor the coordinates are given, hence we used the few indicated topographic features (islands) and the sediment core locations to take into account a summer ice edge north of the Barents Sea in our sea-ice mask. We mention this in Section 2.1 of the revised manuscript.

65 is associate with ⟶ associated with

Corrected

72-73 the magnitude of the data (anomalies) themselves as well as on the gradients, the variability and data-analysis misfits

Rewritten as follows: "the magnitude of the data (anomalies) themselves as well as on the gradients, the variability and data-analysis misfits"

82 We fitted the covariance function to the foraminiferal data ⟶ indicate how many data points were considered for the fit.

There were 444 data points considered for the fit. We added this number to the revised manuscript.

84 estimates of the correlation length of 9.2° and 10.2° ⟶ is there a physical explanation to this difference, or do you attribute that to numerics?

We now attributed this difference to the overall larger data covariance for July-August-September (JAS), resulting in a slightly larger correlation length than for January-February-March (JFM).

94 To each sea-ice covered data point we assigned an error of 2 °C ⟶ is it necessary, since you defined a coastline and mask using "glacial topography GLAC-1D"

Please see our response to your general comment on lines 94–94.

103: new (artificial) diatom and radiolaria data ⟶ what is the source of these data? (and why "artificial"?)

The diatom and radiolarian data for JAS are "artificial" in the sense that they were generated from the results of the first step of the DIVA analysis at the grid points where diatom and radiolaria data for JFM only exist (please see our response to your general comment on lines 89–109).

141 South Alantic ⟶ South Atlantic

Corrected

169-170 DIVA may be used to more accurately estimate the spatial covariances as described by the non-diagonal terms ⟶ Beckers et al. (2014) may be relevant for this aspect Beckers, J.-M.; Barth, A.; Troupin, C. & Alvera-Azcárate, A. Some approximate and efficient methods to assess error fields in spatial gridding with DIVA (Data Interpolating Variational Analysis) (2014). Journal of Atmospheric and Oceanic Technology, 31: 515-530. doi:10.1175/JTECH-D-13-00130.1

Thank you for pointing out this reference to us. We included it in the revised manuscript.

224 may allow to first smooth ⟶ may allow one to first smooth

Corrected

Figure 2:

- *indicate the meaning of the yellow-brownish area close to the Antarctica (rectangles in the attached figure)*

  We apologize for the missing information in the figure caption. The yellow-brownish areas close to Antarctica and in the Arctic ocean indicate the LGM sea-ice masks based on the selected LGM sea-ice reconstructions.

- *Analyzed SST anomalies ⟶ with respect to what reference or background are computed the anomalies? (also in text, line 97).*

  The LGM estimates from the MARGO database are themselves anomalies that are calculated with respect to World Ocean Atlas 1998. We will clarify this in the Methods section of the revised manuscript.

- *the size of the dots representing the data is a little bit to large, so several dots overlap, especially in the northern part of the domain. In Figure 4 the dots are smaller.*

  Thank you for pointing this out to us. In the final version of the manuscript, we will reduce the size of the dots representing the data and use the same size in all figures.

334 WOA: World Ocean Atlas 1998 ⟶ why not use a more recent version of the World Ocean Atlas?

The main reason for using the 1998 version of the World Ocean Atlas is to be consistent with the MARGO database, because it is this version that was used for calibrating the methods which were used to reconstruct the LGM estimates and served as a reference for the LGM SST anomalies. Furthermore, the majority of the data that entered the 1998 version represents observations that were taken before the intensification of global warming towards the end of the 20^{th} century, thereby reducing the anthropogenic imprint.

Figures for the monthly fields: having 6 (or maybe 12) sub-figures seems possible and won't cause problem to the readability of the plots.

Thank you fo this suggestion. In the final version of the manuscript, we will try combining 6 or even 12 sub-plots in one figure and check its readability, especially of the dots representing the data.

References

Abelmann, A. and Gersonde, R.: Biosiliceous particle flux in the Southern Ocean, Marine Chemistry, 35, 503–536, 1991.

Broccoli, A. J. and Marciniak, E. P.: Comparing simulated glacial climate and paleodata: A reexamination, Paleoceanography, 11, 3–14, 1996.

CLIMAP Project Members: The Surface of the Ice-Age Earth, Science, 191, 1131, https://doi.org/10.1126/science.191.4232.1131, 1976.

CLIMAP Project Members: Seasonal reconstructions of the Earth's surface at the Last Glacial Maximum, Geological Society of America, Map and Chart Series, MC-36, 1–18, 1981.

Fischer, G., Gersonde, R., and Wefer, G.: Organic carbon, biogenic silica and diatom fluxes in the marginal winter sea ice zone and in the Polar Front Region in the Southern Ocean (Atlantic sector): interannual variation and changes in composition, Deep-Sea Research II, 49, 1721–1745, https://doi.org/10.1016/S0967-0645(02)00009-7, 2002.

Gersonde, R. and Zielinski, U.: The reconstruction of late Quaternary Antarctic sea-ice distribution –the use of diatoms as proxies for sea-ice, Paleogeography, Paleoclimatology and Paleoecology, 162, 263–286, https://doi.org/10.1016/S0031-0182(00)00131-0, 2000.

Gersonde, R., Crosta, X., Abelmann, A., and Armand, L.: Sea-surface temperature and sea ice distribution of the Southern Ocean at the EPILOG Last Glacial Maximum – a circum-Antarctic view based on siliceous microfossil records, Quaternary Science Reviews, 24, 869–896, https://doi.org/doi:10.1016/j.quascirev.2004.07.015, 2005.

Manabe, S. and Broccoli, A. J.: Beyond Global Warming, Princeton University Press, https://doi.org/10.1515/9780691185163, 2020.

Paul, A. and Schäfer-Neth, C.: Modeling the water masses of the Atlantic Ocean at the Last Glacial Maximum, Paleoceanography, 18, doi:10.1029/2002PA000 783, 2003.

Pflaumann, U., Sarnthein, M., Chapman, M., Funnel, B., Huels, M., Kiefer, T., Maslin, M., Schulz, H., Swallow, J., van Kreveld, S., Vautravers, M., Vogelsang, E., and Weinelt, M.: The Glacial North Atlantic: Sea-surface conditions reconstructed by GLAMAP-2000, Paleoceanography, 18, doi:10.1029/2002PA00 774, 2003.

PMIP: Paleoclimate Modelling Intercomparison Project, http://www-pcmdi.llnl.gov/pmip/newsletters/newsletter02.html, Tech. rep., 1993.

Sarnthein, M., Gersonde, R., Niebler, S., Pflaumann, U., Spielhagen, R., Thiede, J., Wefer, G., and Weinelt, M.: Overview of Glacial Atlantic Ocean Mapping (GLAMAP 2000), Paleoceanography, 18, doi:10.1029/2002PA00 769, 2003.

Schäfer-Neth, C. and Paul, A.: The Atlantic Ocean at the Last Glacial Maximum: 1. Objective mapping of the GLAMAP sea-surface conditions, in: The South Atlantic in the Late Quaternary: Reconstruction of Material Budgets and Current Systems, edited by Wefer, G., Mulitza, S., and Ratmeyer, V., pp. 531–548, Springer-Verlag, Berlin, Heidelberg, 2004.

Schäfer-Neth, C., Paul, A., and Mulitza, S.: Perspectives on mapping the MARGO reconstructions by variogram analysis/kriging and objective analysis, Quaternary Science Reviews, 23, 1083–1093, doi:10.1016/j.quascirev.2004.06.017, 2005.

Troupin, C., Barth, A., Sirjacobs, D., Ouberdous, M., Brankart, J.-M., Brasseur, P., Rixen, M., Alvera-Azcárate, A., Belounis, M., Capet, A., Lenartz, F., Toussaint, M.-E., and Beckers, J.-M.: Generation of analysis and consistent error fields using the Data Interpolating Variational Analysis (DIVA), Ocean Modelling, 52-53, 90–101, https://doi.org/10.1016/j.ocemod.2012.05.002, http://modb.oce.ulg.ac.be, 2012.

WOA: World Ocean Atlas 1998, Tech. rep., National Oceanographic Data Center, Silver Spring, Maryland, 1998.

Xiao, X., Stein, R., and Fahl, K.: MIS 3 to MIS 1 temporal and LGM spatial variability in Arctic Ocean sea ice cover: Reconstruction from biomarkers, Paleoceanography, 30, 969–983, https://doi.org/10.1002/2015PA002814, 2015.

A global climatology of the ocean surface during the Last Glacial Maximum mapped on a regular grid (GLOMAP) – Final response to referee comments

André Paul[1], Stefan Mulitza[1], Ruediger Stein[1, 2], and Martin Werner[2]

[1] MARUM – Center for Marine Environmental Sciences and Department of Geosciences, University of Bremen, Bremen, Germany

[2]Alfred Wegener Institute, Helmholtz Centre for Polar and Marine Research (AWI), Bremerhaven, Germany

Response to Referee #2 (Jessica Tierney)

We are thankful to the referee for her insightful comments which we feel will substantially improve our manuscript.

General comments

Paul et al. present a spatial reconstruction of LGM SST anomalies and sea-ice ex- tent using a new interpolation method, DIVA. Since the underlying data is mostly the MARGO data, the authors get generally the same results as MARGO (2009), with perhaps even smaller anomalies for glacial cooling. I have a couple of general comments here about the data and method used:

1) Underlying data. The sea-ice reconstruction appears to be based on both faunal assemblages and biomarker evidence like IP25, but the SST reconstruction is based only on faunal data from the MARGO collection. Why is this? I'm not sure why the authors would not use the geochemical data in the MARGO collection (?) If there is a reason, then it should be made clear. There is arguably value in a single-proxy field reconstruction, but it should be justified. Also, I think some of the faunal data may have no-analog issues. Were these dealt with in any way?

We agree that we should make clear why we base the gridded SST on the faunal and floral data only, which we now summarize in the revised discussion (p. 10–11 of the revised manuscript). In fact, there are a number of reasons:

- Our interest is in a monthly climatology of the SST anomaly and sea-ice extent during the LGM, and while faunal and floral assemblages are not without issues, they are the only sedimentary proxy that can provide a seasonal reconstruction.
- In addition, a single-proxy reconstruction has the advantage of internal consistency between the different sediment core sites, thereby reducing the noise.
- As for the MARGO reconstruction of the northern North Atlantic Ocean, all four proxies (planktonic foraminifer assemblages, dinocyst assemblages, alkenone coccolithophorid biomarkers and Mg/Ca ratios in planktonic forminifers) support the same features of sea-ice cover (de Vernal et al., 2006; see also Sarnthein et al., 2003b). The IP25/PIP25

data by Xiao et al. (2015, Fig. 7a) and Méheust et al. (2018) add information for the Barents Sea and the North Pacific Ocean, respectively. However, in the Nordic Seas, there are large discrepancies between the different SST reconstructions, well above their level of uncertainties (de Vernal et al., 2006). We suspect that the apparently warm signal recorded by dinocyst assemblages, coccolithophores and alkenones may be due to long-distance lateral transport (de Vernal et al., 2006; Rühlemann and Butzin, 2006), whereas foraminifera-based proxies have the advantage that they drop very quickly to the sediment (Takahashi and Be, 1984). Further possible sources of errors are the overwintering of dinoflagellates in a cyst phase as well as their broad tolerances for temperature (Dale, 2001). Using alkenones for SST reconstructions might be problematic in high latitudes because of the low sensitivity of the calibration of alkenones at low temperature (Conte et al., 2006), the possibility of redeposition of old and warm signal carrying alkenones with particulate matter originating from the glaciated continental margins and once more the influence of alkenones transported by currents from warmer areas into the polar regions (e.g., Bendle and Rosell-Melé, 2004; Filippova et al., 2016).

- Furthermore, foraminiferal assemblages are usually dominated by species adapted to the environment of the overlying water column (Morey et al., 2005). We therefore consider the temperature estimation to be more robust against the expatriation of single shells that can affect proxies measured on monospecific samples.

- Finally, proxies based on the chemistry of shells of living organisms suffer from the inherent problem that the environmental sensitivity of that organism biases the recording of the proxy (Mix, 1987; Fraile et al., 2009). The transfer function method does not have this problem since it actually uses the environmental sensitivity of foraminifera.

The MARGO project carefully dealt with the no-analog problem in a number of ways. For example, Gersonde et al. (2005) discard all samples with no analogs (dissimilarity > 0.25) and when the majority of the samples in the LGM interval has no anlogs, the estimated quality level is downgraded to 3. Kucera et al. (2005) combine three methods (Artificial Neural Networks – ANN, Revised Analog Method – RAM, Maximum Similarity Technique – SIMMAX) in a multi-technique approach that facilitates a test of the robustness of SST estimates and provides a means to identify potential no-analog conditions or faunas.

A bigger problem with the choice of data is that MARGO is over a decade old now, and surely there have been more faunal datasets published since then (Certainly, there is far more geochemical data available now). Since the authors just use the MARGO data, they get results that nearly the same as MARGO. This doesn't seem like an advance in our understanding of the LGM. If the purpose of this paper is provide new insights into the LGM, I would suggest that the authors consider updating their dataset. If the purpose of this paper is to demonstrate a method (DIVA) then the cooling and ECS results should be downplayed.

An important purpose of our manuscript is indeed to demonstrate the applicability of DIVA to sparse and irregularly spaced paleoceanographic data. As we now point out in the Outlook section of the revised manuscript (p. 14), an update of MARGO is certainly important, however, it is beyond the scope of our current work.

We agree that we cannot expect to find truly new results, but we actually see a number of advantages using the well-established MARGO database: To date, it still provides the most comprehensive dataset of LGM SST anomalies at the sediment core locations including their error estimates. Without creating a spatially complete, gridded climatology the MARGO project

has not been able to provide area- and uncertainty-weighted global and regional averages or boundary conditions. The main motivation of our manuscript is to provide a spatially complete, continuous gridded climatology for such purposes. By using MARGO, we can directly compare the gridded and non-gridded data and assess the effect of proper weighting in calculating global and regional averages, and we indeed find small but noticeable differences.

Another advantage of the MARGO database is the consistent use of the modern SST (WOA, 1998) as the calibration as well as the reference dataset. Most methods used for temperature reconstruction are calibrated to absolute temperatures, not temperature differences or changes. By using the calibration dataset as a reference dataset, any error is only incurred once in calculating the LGM anomaly. If using any other time slice (e.g., the Late Holocene) as a reference dataset, the error would double.

With respect to downplaying the cooling and ECS results, please see our response to the major point no. 4.

2) DIVA method. This method is new to me, but seems appropriate for the problem at hand. However some more description of the method is needed here for non-specialists. I'm also wondering, given that DIVA was designed to work with more dense modern oceanographic data, how well it does with the sparse data of the LGM? Can the authors do some validation tests to assess this? E.g., withhold 10-25% of the data, fit the field using DIVA, then validate on the withheld data? This would provide some sense of performance.

Thank you for suggesting this useful test, which we now provide in the revised manuscript (p. 6 and p. 8) to give an idea of the performance, together with some more explanation of the method for non-specialists. For the test, we adopted the procedure by Schäfer-Neth et al. (2005), which allowed us compare our results to variogram analysis and kriging and the Levitus objective analysis.

3) Comparisons to other field reconstructions of the LGM. The authors discuss how their result is fairly similar to MARGO, which is not surprising since the underlying data are similar. What about other products? There are some data assimilation prod- ucts to compare with (Annan and Hargreaves, 2013) - Paul is a co-author on one of them (Kurahaski-Nakamura et al., 2017 https://doi.org/10.1002/2016PA003001) and see also Amrhein et al., 2018 (https://doi.org/10.1175/JCLI-D-17-0769.1). We have a new data assimilation product available as well (in review, but a preprint is available here: https://eartharxiv.org/me5uj/) based on an updated database of geochemical proxies.

Thank you for this valuable suggestion, too. In the revised manuscript, we follow up on it and compare our gridded climatology with the products by Annan and Hargreaves (2013), Kurahashi-Nakamura et al. (2017b) and Tierney et al. (2020) as well as by CLIMAP (1981) and GLAMAP (Sarnthein et al., 2003a) (Tables 3 and 4 and Figure 6), and we mention the advantages and disadvantages of the various methods. For example, while DIVA is a purely statistical method, the adjoint method used by Kurahashi-Nakamura et al. (2017a) (as well as Amrhein et al. (2018)) makes use of the physics and paramaterizations of an ocean general circulation model (MITgcm), however, it also inherits the biases of this model. In contrast, Annan and Hargreaves (2013) employ an ensemble of models, but with partly inconsistent physics and parameterizations.

4) Estimates of glacial cooling and climate sensitivity. In keeping with the MARGO results, these are arguably unrealistically low (global SST change of -1.7, ECS of 1.5). The MARGO-based results of ECS (Schmittner et al. 2011) have faced a lot of criticism. Multiple studies have suggested a global SST change closer to -3C (Ballantyne et al., 2005, Lea et al., 2000) and a

corresponding global air temperature change closer to 5-6C (e.g. Snyder, 2016, Nature; Schneider von Deimling et al., 2006 GRL, Holden et al., 2010 Climate Dynamics, Bereiter et al., 2018, Nature, and our new estimate in our preprint noted above). There needs to be a critical discussion in light of these other results.

According to Bindoff et al. (2013), the equilibrium climate sensitivity is likely in the range of 1.5 °C to 4.5 °C ("high confidence"), extremely unlikely less than 1°C ("high confidence"), and very unlikely greater than 6°C ("medium confidence"). The PALAEOSENS Project Members (2012) estimate based on a comprehensive set of reconstructions of past temperatures and radiative forcing yields a range of 2.2 °C to 4.8°C for the actual climate sensitivity. If taken at face value, our result would imply a value of the equilibrium climate sensitivity at the low end of the classical range. While neither a value of the equilibrium climate sensitivity at the low end (about 1.5 °C) nor at the high end (about 4.5 °C) can be ruled out beforehand, we agree that a critical discussion of our estimate, in the light of these results, and especially the new results by Judd et al. (2020), Sherwood et al. (2020) and Tierney et al. (2020), is needed. In an attempt to provide a balanced view and avoid a simplistic approach, we extended and largely rewrote the Discussion (p. 10–13) and Conclusions (p. 13–14) sections in the revised manuscript.

Regarding the study by Schmittner et al. (2011), it was mainly criticized because of some methodological issues (e.g., missing atmospheric feedbacks, a definition of climate sensitivity that includes feedbacks associated with vegetation, an insufficiently steep lapse rate, underprediction of land temperatures and misfit of ocean data in mid- and high latitudes – see the discussion in RealClimate, 2011). These resulted in a global cooling during the LGM in the range of 1.7 °C to 3.7 °C, which appears to be too small and possibly led to an underestimate of the climate sensitivity with a surprisingly low uncertainty range of 1.4 °C to 2.8 °C. Indeed, Annan and Hargreaves (2013), who also used MARGO as ocean data, arrived at a larger global cooling during the LGM of 3.1 °C to 4.7 °C, supposedly implying a larger climate sensitivity.

The best resolved alkenone-based SST estimates from the central Pacific show an SST change between 1.2 °C and 2 °C (Prahl et al., 1989; Lee et al., 2001; de Garidel-Thoron et al., 2007). From a number of studies using Mg/Ca as well as alkenones, Lea (2004) finds a tropical cooling at the LGM by 2.8 °C $\pm$ 0.7 °C. Leduc et al. (2017) summarize the results of the Sensitivity of the Tropics (SENSETROP) working group, which after the incorporation of high-quality records and a thorough quality control obtains a cooling of the low latitudes during the LGM of -2.3 °C $\pm$ 0.8 °C and -2.4 °C $\pm$ 0.8°C for alkenone- and Mg/Ca-based SST estimates, respectively. Tierney et al. (2020) obtain a very similar mean tropical cooling of -2.5 °C (-2.8 °C to -2.2 °C, 95 % CI) from the SST proxies on their own. These values are indeed larger than the estimates by CLIMAP, MARGO and Annan and Hargreaves (2013) by up to a degree, but not as large as the early estimate from corals by Guilderson et al. (1994) of about 5 °C, which made Crowley (2000) wonder whether it would be possible for corals to survive in the tropical ocean at such low temperatures. The assimilated mean tropical cooling by Tierney et al. (2020) is -3.9 °C (-4.2 °C to -3.7 °C, 95 % CI), which is larger than the data-only estimates that may suffer from incomplete and uneven sampling.

Regarding faunal assemblages, Ravelo et al. (1990) demonstrate that in the equatorial Atlantic they do not respond primarily to SST, but rather to thermocline and seasonality changes. Along similar lines, Telford et al. (2013) provide evidence that planktonic foraminifera assemblages can be more sensitive to subsurface temperatures than the 10-m SST that they are usually calibrated against, e.g., as in MARGO. They conclude that reconstructions of 10-m SST are likely to be biased, with the sign

and magnitude of the bias varying regionally, probably causing a warm bias in the tropical North Atlantic, but foraminifera-based reconstructions for other ocean basins still remaining to be assessed

In our revised manuscript, we took up the above discussion and commented on why our estimate of the global SST decrease based on the MARGO faunal and floral assemblages may be at the low end of the currently accepted range (p. 11–12 of the revised manuscript).

Also: how was ECS calculated? There must be a scaling assumption to translate to global mean surface temperature, and then there has to be estimation of the forcing as well (the denominator). Please describe this.

We used the same simple linear relationship as MARGO Project Members (2009), which is shown in Fig. 6 by Schneider von Deimling et al. (2006), but we now refer to the excellent recent review by Sherwood et al. (2020), too (lines 374–389 of the revised manuscript).

My overall take of this paper is: It's really interesting to see the application of DIVA to paleoclimate information, and this could use some more discussion and exploration (perhaps comparison to optimal interpolation). However in terms of providing new scientific insights into the LGM, the paper is limited here by use of the MARGO faunal dataset, which ultimately shapes the results. No matter what the method used, the MARGO data, particularly the assemblage data, provide an estimate of glacial cooling that is very small. This result has been challenged a lot over the years and there is a sense that perhaps no-analog problems still plague the faunal data.

I think the best solution here would be to update the underlying dataset with new studies - either new faunal data or new faunal data + geochemical data. Otherwise, the conclusions of the paper re: glacial cooling and climate sensitivity are just the same as MARGO.

Alternatively, the authors could treat this paper as a methods paper. If the goal is to just demonstrate application of DIVA, then it's OK to stick with MARGO. But in that case comparisons should be made with other field estimation methods (OI, data as- similation) and the scientific results (LGM cooling and ECS) should be downplayed and presented critically since they are ultimately tied to the underlying data.

We agree to elaborate more on the DIVA method and included a test of this method on a subset of the data. Updating the MARGO data with new data sets is unfortunately beyond the scope of the current manuscript and must be deferred to a new project. We put the values of the LGM cooling and ECS, now based on a properly area- and uncertainty-weighted gridded climatology, in perspective, comparing them to values obtained from other data and different methods.

Specific comments:

Abstract: Clarify that GLOMAP is based on only faunal transfer function data (except for the use of IP25 for sea ice).

Agreed (line 3 of the revised manuscript)

Section 2.1: Please clarify here what each reconstruction is based on (transfer functions, IP25, etc).

Agreed (lines 59-63 and line 65 of the revised manuscript)

Section 2.2: Why did you only use the faunal data from the MARGO collection? Also MARGO is now 11 years old. I imagine that more data have been published since then. Certainly for the geochemical proxies this is true. I think it's worth updating the data with newly published results.

See our response the major point no. 1

Section 2.3: This section could benefit from a little more explanation of how DIVA works since most readers will not be familiar with Troupin et al. (2012). In particular, it would be useful to describe how DIVA is distinct from pure interpolation (no information about spatial relationships) vs. optimal interpolation (covariance structure is set). Is DIVA essentially isotropic away from the coastlines?

Thank you for bringing up this point. We added to the manuscript that DIVA indeed makes use of information on spatial relationships (lines 99-102 of the revised manuscript). In our application, it is essentially isotropic away from the coastlines, however, in principle, if current velocities are known, an advective constraint may be imposed, too.

Section 3.1: The use of past tense here is a little confusing. Use present tense for describing the results.

Generally, we would like to adhere to the rule of describing our own results in past tense and referring to other published results in present tense.

References

Amrhein, D. E., Wunsch, C., Marchal, O., and Forget, G.: A Global Glacial Ocean State Estimate Constrained by Upper-Ocean Temperature Proxies, Journal of Climate, 31, 8059–8079, https://doi.org/10.1175/JCLI-D-17-0769.1, 2018.

Annan, J. D. and Hargreaves, J. C.: A new global reconstruction of temperature changes at the Last Glacial Maximum, Climate of the Past, 9, 367–376, https://doi.org/10.5194/cp-9-367-2013, 2013.

Bendle, J. and Rosell-Melé, A.: Distributions of UK37 and UK´37 in the surface waters and sediments of the Nordic Seas: Implications for paleoceanography, Geochemistry, Geophysics, Geosystems, 5, https://doi.org/10.1029/2004GC000741, 2004.

Bindoff, N. L., Stott, P. A., AchutaRao, K. M., Allen, M. R., Gillett, N., Gutzler, D., Hansingo, K., Hegerl, G., Hu, Y., Jain, S., Mokhov, I. I., Overland, J., Perlwitz, J., Sebbari, R., and Zhang, X.: Detection and Attribution of Climate Change: from Global to Regional, in: Climate Change 2013: The Physical Science Basis. Contribution of Working Group I to the Fifth Assessment Report of the Intergovernmental Panel on Climate Change, edited by Stocker, T., Qin, D., Plattner, G.-K., Tignor, M., Allen, S., Boschung, J., Nauels, A., Xia, Y., Bex, V., and Midgley, P., Cambridge University Press, Cambridge, United Kingdom and New York, NY, USA, 2013.

CLIMAP Project Members: Seasonal reconstructions of the Earth's surface at the Last Glacial Maximum, Geological Society of America, Map and Chart Series, MC-36, 1–18, 1981.

Conte, M. H., Sicre, M.-A., Rühlemann, C., Weber, J. C., Schulte, S., Schulz-Bull, D., and Blanz, T.: Global temperature calibration of the alkenone unsaturation index (UK′37) in surface waters and comparison with surface sediments, Geochemistry, Geophysics, Geosystems, 7, Q02 005, https://doi.org/10.1029/2005GC001054, 2006.

Crowley, T.: CLIMAP SSTs re-revisited, Climate Dynamics, 16, 241–255, 2000.

Dale, B.: The sedimentary record of dinoflagellate cysts: Looking back into the future of phytoplankton blooms, Scientia Marina, 65, 257–272, 2001.

de Garidel-Thoron, T., Rosenthal, Y., Beaufort, L., Bard, E., Sonzogni, C., and Mix, A. C.: A multiproxy assessment of the western equatorial Pacific hydrography during the last 30 kyr, Paleoceanography, 22, https://doi.org/10.1029/2006PA001269, 2007.

de Vernal, A., Rosell-Melé, A., Kucera, M., Hillaire-Marcel, C., Eynaud, F., Weinelt, M., Dokken, T., and Kageyama, M.: Comparing proxies for the reconstruction of LGM sea-surface conditions in the northern North Atlantic, Quaternary Science Reviews, 25, 2820–2834, https://doi.org/10.1016/j.quascirev.2006.06.006, 2006.

Filippova, A., Kienast, M., Frank, M., and Schneider, R. R.: Alkenone paleothermometry in the North Atlantic: A review and synthesis of surface sediment data and calibrations, Geochemistry, Geophysics, Geosystems, 17, 1370–1382, https://doi.org/10.1002/2015GC006106, 2016.

Fraile, I., Mulitza, S., and Schulz, M.: Modeling planktonic foraminiferal seasonality: Implications for sea-surface temperature reconstructions, Marine Micropaleontology, 72, 1–9, https://doi.org/10.1016/j.marmicro.2009.01.003, 2009.

Gersonde, R., Crosta, X., Abelmann, A., and Armand, L.: Sea-surface temperature and sea ice distribution of the Southern Ocean at the EPILOG Last Glacial Maximum – a circum-Antarctic view based on siliceous microfossil records, Quaternary Science Reviews, 24, 869–896, https://doi.org/doi:10.1016/j.quascirev.2004.07.015, 2005.

Guilderson, T. P., Fairbanks, R. G., and Rubenstone, J. L.: Tropical Temperature Variations Since 20,000 Years Ago: Modulating Interhemispheric Climate Change, Science, 263, 663–665, https://doi.org/10.1126/science.263.5147.663, 1994.

Judd, E. J., , Bhattacharya, T., and Ivany, L. C.: A Dynamical Framework for Interpreting Ancient SeaSurface Temperature, Geophysical Research Letters, 47, e2020GL089 044, https://doi.org/10.1029/2020GL089044, 2020.

Kucera, M., Weinelt, M., Kiefer, T., Pflaumann, U., Hayes, A., Weinelt, M., Chen, M.-T., Mix, A. C., Barrows, T. T., Cortijo, E., Duprat, J., Juggins, S., and Waelbroeck, C.: Reconstruction of sea-surface temperatures from assemblages of planktonic foraminifera: Multi-technique approach based on geographically constrained calibration data sets and its application to glacial Atlantic and Pacific Oceans, Quaternary Science Reviews, 24, 951–998, https://doi.org/doi:10.1016/j.quascirev.2004.07.014, 2005.

Kurahashi-Nakamura, T., Paul, A., and Losch, M.: Dynamical reconstruction of the global ocean state during the Last Glacial Maximum, Paleoceanography, 32, 326–350, https://doi.org/10.1002/2016PA003001, 2017a.

Kurahashi-Nakamura, T., Paul, A., and Losch, M.: Dynamical reconstruction of the global ocean state during the Last Glacial Maximum, Paleoceanography, 32, 326–350, https://doi.org/10.1002/2016PA003001, 2017b.

Lea, D. W.: The 100,000-yr Cycle in Tropical SST, Greenhouse Forcing, and Climate Sensitivity, Journal of Climate, 17, 2170–2179, 2004.

Leduc, G., de Garidel-Thoron, T., Kaiser, J., Bolton, C., and Contoux, C.: Databases for sea surface paleotemperature based on geochemical proxies from marine sediments: implications for model-data comparisons, Quaternaire, 28, 201–216, https://doi.org/10.4000/quaternaire.8034, http://quaternaire.revues.org/8034, 2017.

Lee, K. E., Slowey, N. C., and Herbert, T. D.: Glacial sea surface temperatures in the subtropical North Pacific: A comparison of $U_{37}^{k'}$, $\delta^{18}O$, and foraminiferal assemblage temperature estimates, Paleoceanography, 16, https://doi.org/10.1029/1999PA000493, 2001.

MARGO Project Members: Constraints on the magnitude and patterns of ocean cooling at the Last Glacial Maximum, Nature Geoscience, 2, 127–132, https://doi.org/doi:10.1039/NGEO411, 2009.

Méheust, M., Ruediger Stein, R., Fahl, K., and Gersonde, R.: Sea-ice variability in the subarctic North Pacific and adjacent Bering Sea during the past 25 ka: new insights from IP25 and $U_{37}^{k'}$ proxy records, Arktos, 4, https://doi.org/10.1007/s41063-018-0043-1, 2018.

Mix, A. C.: The oxygen-isotope record of glaciation, in: North America and adjacent oceans during the last deglaciation, edited by Ruddiman, W. F. and Wright, Jr., H. E., vol. K-3 of *The Geology of North America*, Geological Society of America, Boulder, Colorado, https://doi.org/10.1130/DNAG-GNA-K3.111, 1987.

Morey, A. E., Mix, A. C., and Pisias, N. G.: Planktonic foraminiferal assemblages preserved in surface sediments correspond to multiple environmental variables, Quaternary Science Reviews, 24, 925–950, https://doi.org/10.1016/j.quascirev.2003.09.011, 2005.

PALAEOSENS Project Members: Making sense of palaeoclimate sensitivity, Nature, 491, 683–691, https://doi.org/10.1038/nature11574, 2012.

Prahl, F. G., Muehlhausen, L. A., and Lyle, M.: An organic geochemical assessment of oceanographic conditions at Manop Site C over the past 26,000 years, Paleoceanography, 4, 495–510, https://doi.org/10.1029/PA004i005p00495, 1989.

Ravelo, A. C., Fairbanks, R. G., and Philander, S. G. H.: Reconstructing tropical Atlantic hydrography using planktonic foraminifera and an ocean model, Paleoceanography, 5, 409–431, https://doi.org/DOI: 10.1029/PA005i003p00409, 1990.

RealClimate: Ice age constraints on climate sensitivity, http://www.realclimate.org/index.php/archives/2011/11/ice-age-constraints-on-climate-sensitivity, 2011.

Rühlemann, C. and Butzin, M.: Alkenone temperature anomalies in the Brazil-Malvinas Confluence area caused by lateral advection of suspended particulate material, Geochemistry, Geophysics, Geosystems, 7, Q10 015, https://doi.org/10.1029/2006GC001251, 2006.

Sarnthein, M., Gersonde, R., Niebler, S., Pflaumann, U., Spielhagen, R., Thiede, J., Wefer, G., and Weinelt, M.: Overview of Glacial Atlantic Ocean Mapping (GLAMAP 2000), Paleoceanography, 18, doi:10.1029/2002PA00 769, 2003a.

Sarnthein, M., Pflaumann, U., and Weinelt, M.: Past extent of sea ice in the northern North Atlantic inferred from foraminiferal paleotemperature estimates, Paleoceanography, 18, https://doi.org/10.1029/2002PA00771, 2003b.

Schäfer-Neth, C., Paul, A., and Mulitza, S.: Perspectives on mapping the MARGO reconstructions by variogram analysis/kriging and objective analysis, Quaternary Science Reviews, 23, 1083–1093, doi:10.1016/j.quascirev.2004.06.017, 2005.

Schmittner, A., Urban, Nathan, M., Shakun, J. D., Mahowald, N. M., Clark, P. U., Bartlein, P. J., Mix, A. C., and Rosell-Melé, A.: Climate Sensitivity Estimated from Temperature Reconstructions of the Last Glacial Maximum, Science, 334, 1385–1388, https://doi.org/10.1126/science.1203513, 2011.

Schneider von Deimling, T., Held, H., Ganopolski, A., and Rahmstorf, S.: Climate sensitivity estimated from ensemble simulations of glacial climate, Climate Dynamics, 27, 149–163, doi:10.1007/s00 382–006–0126–8, 2006.

Sherwood, S., Webb, M. J., Annan, J. D., Armour, K. C., Forster, P. M., Hargreaves, J. C., Hegerl, G., Klein, S. A., Marvel, K. D., Rohling, E. J., Watanabe, M., Andrews, T., Braconnot, P., Bretherton, C. S., Foster, G. L., Hausfather, Z., Heydt, A. S. v. d., Knutti, R., Mauritsen, T., Norris, J. R., Proistosescu, C., Rugenstein, M., Schmidt, G. A., Tokarska, K. B., and Zelinka, M. D.: An assessment of Earth's climate sensitivity using multiple lines of evidence, Reviews of Geophysics, p. e2019RG000678, https://doi.org/10.1029/2019RG000678, 2020.

Takahashi, K. and Be, A. W. H.: Planktonic foraminifera: factors controlling sinking speeds, Deep Sea Research Part A. Oceanographic Research Papers, 31, 1477–1500, https://doi.org/10.1016/0198-0149(84)90083-9, 1984.

Telford, R. J., Li, C., and Kucera, M.: Mismatch between the depth habitat of planktonic foraminifera and the calibration depth of SST transfer functions may bias reconstructions, Climate of the Past, 9, 859–870, https://doi.org/10.5194/cp-9-859-2013, 2013.

Tierney, J. E., Zhu, J., King, J., Malevich, S. B., Hakim, G. J., and Poulsen, C. J.: Glacial cooling and climate sensitivity revisited, Nature, 584, 569–573, https://doi.org/10.1038/s41586-020-2617-x, 2020.

WOA: World Ocean Atlas 1998, Tech. rep., National Oceanographic Data Center, Silver Spring, Maryland, 1998.

Xiao, X., Stein, R., and Fahl, K.: MIS 3 to MIS 1 temporal and LGM spatial variability in Arctic Ocean sea ice cover: Reconstruction from biomarkers, Paleoceanography, 30, 969–983, https://doi.org/10.1002/2015PA002814, 2015.

A global climatology of the ocean surface during the Last Glacial Maximum mapped on a regular grid (GLOMAP)

André Paul[1], Stefan Mulitza[1], Ruediger Stein[1,2], and Martin Werner[2]

[1] MARUM – Center for Marine Environmental Sciences and Department of Geosciences, University of Bremen, Bremen, Germany

[2]Alfred Wegener Institute, Helmholtz Centre for Polar and Marine Research (AWI), Bremerhaven, Germany

Correspondence: André Paul (apaul@marum.de)

Abstract. We present a climatology of the sea-surface temperature (SST) anomaly and the sea-ice extent during the Last Glacial Maximum (LGM, 23,000–19,000 years before present) mapped on a global regular $1°\times1°$ grid. It is an extension of the Glacial Atlantic Ocean Mapping (GLAMAP) reconstruction of the Atlantic SST based on the faunal and floral assemblage data of the Multiproxy Approach for the Reconstruction of the Glacial Ocean Surface (MARGO) project and several recent estimates of the LGM sea-ice extent. Such a gridded climatology is highly useful for the visualization of the LGM climate, calculation of global and regional SST averages and estimation of the equilibrium climate sensitivity, as well as a boundary condition for atmospheric general circulation models. The gridding of the sparse SST reconstruction was done in an optimal way using the Data-Interpolating Variational Analysis (DIVA) software, which takes into account the uncertainty on the reconstruction and includes the calculation of an error field. The resulting Glacial Ocean Map (GLOMAP) confirms the previous findings by the MARGO project regarding longitudinal and meridional SST differences that were greater than today in all oceans. Taken at face value, the estimated global and tropical cooling would imply ~~and~~ an equilibrium climate sensitivity at the lower end of the currently accepted range. However, anticipated changes in seasonality and thermal structure of the upper ocean during the LGM as well as a spatial sampling bias are likely to have shifted these estimates towards lower values.

1 Introduction

Gridded climatologies are useful for a number of purposes, for example, for visualizing present or past climate states, calculating global and regional averages, or evaluating climate models. Regarding the evaluation of climate models, unless data locations and model grid points coincide, we cannot quantify the data-model misfit without any sort of mapping. Thus, sparse data must be mapped onto the model grid by statistical methods (Schäfer-Neth et al., 2005; Marchal and Curry, 2008). Furthermore, a gridded sea-surface temperature (SST) climatology may serve as a boundary condition for atmospheric general circulation models (AGCMs) and enable a model evaluation that does not depend on the quality of a simulated SST climatol-

ogy, allowing for another approach in comparing coupled climate models such as in the Paleo-Model Intercomparison Project (PMIP, e.g., Kageyama et al., 2017).

A climate state of the past that is particularly useful for evaluating climate models is the Last Glacial Maximum (LGM, 19,000 to 23,000 years before present; Mix et al., 2001) cold period: The radiative perturbations due to changes in insolation, greenhouse gases and ice sheets are relatively well defined and the paleo-data coverage is comparitively dense and indicates a large response to the radiative forcing (Jansen et al., 2007; Masson-Delmotte et al., 2013). Previous work on a gridded SST climatology for the LGM includes the Climate: Long range Investigation, Mapping, and Prediction (CLIMAP) project (CLIMAP Project Members, 1981), the Glacial Atlantic Ocean Mapping (GLAMAP) SST reconstruction of the Atlantic SST (Sarnthein et al., 2003a) and the Multiproxy Approach for the Reconstruction of the Glacial Ocean Surface (MARGO) (Kucera et al., 2005a). While CLIMAP and GLAMAP (Paul and Schäfer-Neth, 2003; Schäfer-Neth and Paul, 2004) provide seasonal reconstructions of the Earth's surface at the LGM mapped on a 2° grid, MARGO only performed a "pseudo gridding" by calculating 5° block averages (MARGO Project Members, 2009).

CLIMAP used a subjective analysis procedure (i.e. contouring by hand) to yield the paleoisotherm maps (CLIMAP Project Members, 1976, 1981), which were then digitized on a regular grid (see also Broccoli and Marciniak (1996 and Manabe and Broccoli, 2020). With respect to GLAMAP, different methods were applied: Contouring of the paleotemperature maps was also by hand, and the isotherms were derived by means of visual triangulation from strictly linear interpolation between the SST reconstructions at the irregularly distributed neighbor sites (Sarnthein et al., 2003a; Pflaumann et al., 2003). For gridding, either the digitized isotherms (Paul and Schäfer-Neth, 2003) or the SST reconstructions at the sediment core positions (Schäfer-Neth and Paul, 2004) were objectively interpolated using variogram analysis and kriging in spherical coordinates; and the resulting gridded fields were compared (Schäfer-Neth and Paul, 2004, Fig. 5). The seasonal cycle was constructed following the PMIP (1993) guidelines: A sinusoidal cycle was fitted to the glacial-to-modern anomalies and then the modern monthly SST (taken as 10 m data from the WOA, 1998) was added. The variogram analysis and kriging cannot deal easily with coastlines, for example, it may take into account data points separated by a land bridge or an island. This was one motivation to apply the DIVA method (Troupin et al., 2012), which employs a finite-element mesh derived from a given topography.

Here we present an ocean climatology of the sea surface during the LGM mapped on a global $1° \times 1°$ grid. This Glacial Ocean Map (GLOMAP) extends the gridded GLAMAP climatology to the global ocean based on the MARGO SST reconstruction. In addition, we included a more recent estimate of Southern Ocean summer sea-ice extent (Roche et al., 2012) and reconstructions of Arctic and North Pacific sea-ice extent using the IP25/PIP25 sea-ice proxy and phytoplankton-derived biomarkers (Xiao et al., 2015; Méheust et al., 2016; Méheust et al., 2018). The sparse SST reconstruction, complemented with the reconstructed sea-ice boundaries in the northern and southern hemispheres, was gridded in an optimal way using the Data-Interpolating Variational Analysis (DIVA) method (Troupin et al., 2012). This method allows one to take into account the uncertainty on the (paleo-) data and calculate an uncertainty field, which can be used as a weight in calculating uncertainty-weighted global and regional averages ~~or for assessing the data-analysis mismatch~~. Originally developed for usually much denser oceanographic observations, the DIVA method proved to be capable of analyzing sparse paleo data as well.

2 Methods

2.1 Selecting LGM sea-ice extent reconstructions

For estimating LGM sea-ice extent, we made use of estimates of maximum and minimum sea-ice extent in the Northern and Southern Hemispheres and added a physically reasonable seasonal cycle. As for the MARGO reconstruction of sea-ice extent in the northern North Atlantic Ocean, all four proxies used (planktonic foraminifer assemblages, dinocyst assemblages, alkenone coccolithophorid biomarkers and Mg/Ca ratios in planktonic forminifers) support the same features of sea-ice cover (de Vernal et al., 2006; cf. Sarnthein et al., 2003b). The IP25/PIP25 data by Xiao et al. (2015, Fig. 7a) and Méheust et al. (2018) add information for the Barents Sea and the North Pacific Ocean, respectively. Since there are only few SST reconstructions in the high latitudes of either hemisphere, the information on past sea-ice coverage also served to fill in the gaps.

In line with earlier transfer function results obtained by the GLAMAP project (Sarnthein et al., 2003a), the Nordic Seas were taken as ice-free during summer. Since the sea-ice edges are not provided in digital format, we digitized the curves from the published maps by de Vernal et al. (2005, Fig. 10, upper left) and Kucera et al. (2005b, Fig. 25) for the Labrador Sea and Nordic Seas, Xiao et al. (2015, Fig. 7a) for the Barents Sea and Méheust et al. (2018, Fig. 9a) for the North Pacific Ocean to obtain their location in geographic coordinates. In case of Xiao et al. (2015, Fig. 7a), neither the projection nor the coordinates are given, hence we used the few indicated topographic features (islands) and the sediment core locations to take into account the summer ice edge north of the Barents Sea in our sea-ice mask. Similarly, we digitized sea-ice reconstructions by Gersonde et al. (2005, Fig. 4, maximum extent of winter sea ice "E-LGM-WSI" and sporadic occurrence of summer sea ice "E-LGM-SSI") and Roche et al. (2012, Fig. 4, bottom, Southern Ocean summer sea-ice extent "PROX.") for the Southern Hemisphere. If necessary, we re-projected them (e.g., from a polar stereographic or orthographic projection) to longitude and latitude. We connected them smoothly in each hemisphere and season and created sea-ice masks for summer and winter (note that the sea-ice reconstructions based on IP25/PIP25 by Xiao et al., 2015, and Méheust et al., 2018, apply to spring, but were in this study taken as an approximation to the winter sea-ice edge).

We created a seasonal cycle of sea-ice coverage as follows: At a given longitude, we assumed a sinusoidal cycle of the latitude of the sea ice edge (cf. Eisenman, 2010) between the maximum and minimum sea ice extent in either hemisphere.

2.2 Selecting LGM SST reconstructions

Faunal and floral assemblages still provide the best spatial coverage and they are the only sedimentary proxy that has the potential to provide a seasonal reconstruction. For these reasons, as well as for internal consistency and reduced noise among the individual LGM estimates, we selected from the MARGO database (Kucera et al., 2005a; MARGO Project Members, 2009) only those that were based on the faunal and floral transfer function technique. However, in the Nordic Seas, there are large discrepancies between the different SST reconstructions, well above their level of uncertainties (de Vernal et al., 2006). We therefore used dinocyst assemblages ~~were~~ only ~~used~~ south of the assumed winter sea-ice boundary at about 50°N (de Vernal et al., 2005; de Vernal et al., 2006). To this end, we extracted all dinoflagellate data assumed to be not affected by winter sea-ice cover in the Nordic Seas.

Each MARGO SST estimate is associated with an error that is equal to the product of the calibration error and a semi-quantitative "reliability index". The reliability index takes into account the number of samples, the quality of the age model and a possible lack of stationarity reflecting, for example, possible no-analogue situations and a known regional or sedimentological bias (MARGO Project Members, 2009). The calibration error ranges typically between 1 °C and 1.5 °C, and the reliability index ranges between 1 for high reliability and about 3.3 for low reliability. All errors were taken to reflect a $1\,\sigma$ confidence interval.

2.3 Gridding

We chose DIVA over other methods because it takes the coastlines into account, since the analysis is carried out on a finite-element mesh that is restricted to the sea. This prevents the exchange of information across boundaries such as land bridges, peninsulas or islands, which otherwise might produce artificial mixing between, for example, Pacific and Atlantic water masses across the Panama isthmus. We used version 4.7.1 (doi:10.5281/zenodo.836727) of DIVA (Troupin et al., 2012). The purpose of DIVA is to satisfy a variational principle that includes the magnitude of the data (anomalies) themselves as well as the gradients, the spatial variability and data-analysis misfits (Troupin et al., 2019, Eqs. 2.10 and 2.11). Thus in solving the variational principle, DIVA not only takes into account the distance between analysis and data, but also imposes a smoothness constraint and, if desired, an advection constraint. Moreover, it provides an uncertainty estimate.

The general work flow of DIVA is summarized in Figure 2. The first step is to generate coast lines from a given topography. Based on the resulting coast lines, a finite-element mesh is created, which in our application covers the global ocean including the sea-ice. Then first-guess values of the three analysis parameters (correlation length, signal-to-noise ratio and variance of background field) are estimated and an analytic covariance function is fit to the data, yielding a revised estimate of the correlation length. Finally, a generalized cross validation can be carried out to improve the signal-to-noise ratio and the variance of background field.

To first test the DIVA method on data that are much sparser than oceanographic observations, we adopted the procedure by Schäfer-Neth et al. (2005): We used the annual-mean temperature for 10 m depth from the unanalyzed World Ocean Atlas 1998 data (WOA, 1998), which had also been used to calibrate the MARGO transfer function technique. These temperature data had been averaged to a $2^\circ \times 2^\circ$ regular grid, but otherwise had not been subject to any analysis or interpolation method. The coverage of the unanalyzed data is nearly complete, except for the central Arctic and some points off the Antarctic coast. This allows for a near-global comparison with the results of the interpolation.

The input data set for the DIVA method was created by binning all MARGO core locations in $2^\circ \times 2^\circ$ squares and sampling the $2^\circ \times 2^\circ$ WOA data at these points to reflect the density of the MARGO data. The DIVA method was used to interpolate the sampled points back to the $2^\circ \times 2^\circ$ grid and the annual-mean SST differences between the interpolated and observed fields at all WOA (1998) unanalyzed data locations were calculated as a measure of the misfit.

~~In our case~~To apply the DIVA method to the paleo data, we used the glacial topography GLAC-1D at 21,000 years before present (cf. Tarasov et al., 2012; Briggs et al., 2014) to generate glacial coast lines and create a corresponding global finite-element mesh. The first-guess values of the correlation length and the signal-to-noise ratio were set to 10° and 1.0, respectively. The first-guess value of the variance of the background field was estimated from the foraminiferal SST reconstructions as 6.3

(°C)^2. We fitted the covariance function to the 444 foraminiferal data points for the nominal seasons January-February-March (JFM) and July-August-September (JAS) and obtained estimates of the correlation length of 9.2° and 10.2°, respectively. The data covariance for JAS was overall larger than for JFM, resulting in a slightly larger correlation length. In the remainder of our study, we fixed the correlation length at average value of 10°. The generalized cross validation did not yield significantly different values for the signal-to-noise ratio and the variance of background field. To each data value, we assigned a relative weight, which was inversely proportional to the error (a large value corresponded to a high confidence) and normalized such that the sum over all inverse relative weights equaled the number of data points.

We performed two iterations to create a global gridded climatology of monthly SST. Two iterations were necessary in order to make use of the diatom and radiolarian data from the Southern Ocean, which were only available for Southern Hemisphere summer (JFM), because in this region the biogenic particle flux to the sea floor is restricted to austral summer, even in areas unaffected by sea-ice cover (Abelmann and Gersonde, 1991; Gersonde and Zielinski, 2000; Fischer et al., 2002). Therefore, in the first step, we only used the foraminiferal and dinoflagellate data for JAS and JFM. In the second step, we included the diatom and radiolarian data available for JFM and filled in the missing data for JAS by taking the results from the first step at the grid points where diatom and radiolaria data for JFM exist. In this way we were able to create monthly data at all grid points where data exist and repeat the DIVA analysis:

1. In the first iteration, we concatenated all foraminiferal data and the dinoflagellate data for ice-free regions including their relative weights for JAS and JFM. We created seasonal (monthly) data from the JFM (taken as February) and JAS (taken as August) data using a sine function. We extracted the geographic positions marked as sea ice from the monthly masks of the reconstructed sea-ice extent and determined the local SST anomaly using a temperature of -1.8 °C for the LGM value and the World Ocean Atlas (WOA, 1998) at 10 m depth for the modern value. To each sea-ice covered data point we assigned an error of 2 °C that was chosen to be larger than the error of any individual LGM estimate from the MARGO database to reflect the uncertainty in the LGM sea-ice extent reconstructions. Then we concatenated the seasonal (monthly) foraminiferal and dinoflagellate data and the local SST anomalies from the sea-ice reconstructions and normalized the individual errors such that the sum of all errors equaled one [all SST anomalies are relative to WOA (1998), which was used by MARGO Project Members (2009) for calibrating the methods for estimating the LGM SST values]. Finally, we gridded the data for each month. We achieved continuity across the 0° meridian by adapting the method by Tyberghein et al. (2012) and running two DIVA analyses, one ranging from 0° to 360° (on the "original grid"), the other ranging from -180° to 180° (on a "shifted grid"). The two resulting analyses were combined in one on an output grid that extended from 0° to 360° by calculating a weighted average for each grid point, where the weights were proportional to the zonal distance from the central longitude of the respective input grid.

2. In the second iteration, new (artificial) diatom and radiolaria data for SH winter (JAS) were generated at the grid points where diatom and radiolaria data for SH summer (JFM) exist, either using the anomaly with respect to the present observed SST or the gridded data from iteration 1, depending on whether a grid point was assumed to be ice-covered or ice-free for the LGM. We again created seasonal (monthly) data from the February (JFM) and August (JAS) data using

a sine function and concatenated all the seasonal (monthly) data as before, but now including the diatom and radiolaria data, and we carried out two more DIVA analyses, one for the original and one for the shifted grid. Finally, the two grids were merged once more following the method of Tyberghein et al. (2012).

2.4 Comparison to other reconstructions

For a comparison to previous studies, we calculated the annual-mean anomalies for the global, tropical and high-latitude oceans of the recent reconstructions by Annan and Hargreaves (2013), Kurahashi-Nakamura et al. (2017b) and Tierney et al. (2020) as well as by CLIMAP (1981) and GLAMAP (Sarnthein et al., 2003a) and from our own results. Because an uncertainty estimate was not available for all studies, we only weighted by area.

3 Results

3.1 Test of the DIVA method

Figure A1 shows the coastlines that were generated from the modern topography for testing the DIVA method on the WOA (1998) data sampled at the MARGO core locations, as well as from the LGM topography for our application of the DIVA method to the LGM SST reconstruction. The figure also shows the finite-element meshes based on these coastlines, which exhibit a rather homogeneous resolution.

In Table 1, our results of testing DIVA on a sparse and irregularly spaced subset of WOA (1998) are compared in terms of the root-mean square differences for the different oceans as well as the global ocean by Schäfer-Neth et al. (2005) to two other interpolation methods: variogram analysis and kriging (Deutsch and Journel, 1992) and a variant of objective analysis (Levitus, 1982). Furthermore, Fig. 1 shows a map of the absolute difference that can be directly compared to Fig. 5 by Schäfer-Neth et al. (2005). The regionally averaged results from DIVA turned out to be very similar to those from variogram analysis and kriging and better than those from the Levitus objective analysis. The comparison of Fig. 1 and Fig. 5 by Schäfer-Neth et al. (2005) supports this finding at the local scale: Similar to the variograms and kriging results (Schäfer-Neth et al., 2005, Fig. 5 top), absolute differences were generally small in regions of dense spatial sampling. They became particularly large in the Gulf Stream and Kuroshio regions, because of coarse spatial sampling and (probably) the impact of advection by the western boundary currents, which is missing in our application of DIVA.

3.2 Patterns of LGM SST change

The monthly maps based on the gridded MARGO SST anomaly clearly exhibit the same basic patterns of LGM SST change as the original MARGO Project Members (2009) synthesis (Fig. 3 and Figs. A2 to A9): Generally, the cooling was larger in the Atlantic than in the Pacific and Indian Oceans. There were strong longitudinal and latitudinal differences in all oceans. The cooling was generally larger in the eastern parts of the oceans than in the western parts and was particularly expressed along the coast of Africa, possibly due to an increase in upwelling or an eastward shift of the coastline and the coastal upwelling systems

off Northwest and Southwest Africa (cf. Giraud and Paul, 2010). There was even an 1 °C to 3 °C cooling in the western Pacific warm pool, but overall the east-west temperature differences were less pronounced in the tropical Pacific and Indian Oceans than in the tropical Atlantic Ocean. A 2 °C to 6 °C cooling in the Southern Ocean may indicate a northward migration of the Polar Front. The apparent warming by 1-2°C of the subtropical gyres in the Pacific Ocean was associated with a rather large uncertainty.

3.3 Global and regional mean changes

Annual averages of the gridded monthly values and their uncertainties were calculated as arithmetic means without any weighting. Global and regional averages (Table 2) and zonal averages (Fig. 4) were calculated from the annually-averaged values as weighted means

$$\overline{T} = \frac{\sum_i w_i T_i}{\sum_i w_i}\,, \tag{1}$$

where the weights were given by

$$w_i = \frac{A_i}{u_i^2} \tag{2}$$

with A_i the area of the ith grid cell and u_i the uncertainty of the gridded value in the ith grid cell. The uncertainties of the global and regional averages were estimated as

$$\overline{u} = \sqrt{\sum_i \left(\frac{w_i}{\sum_i w_i} u_i \right)^2} \times f_{\mathrm{inf}}\,. \tag{3}$$

Here the first factor is the simple sum of the local values of the uncertainty of the gridded field that neglects any spatial covariances (i.e., the non-diagonal terms of the covariance matrix), and the second factor is applied to take into account the missing spatial covariances in an approximate way. According to Troupin et al. (2019), the inflation factor

$$f_{\mathrm{inf}} = \sqrt{\frac{4\pi L^2}{\Delta x \Delta y}} \tag{4}$$

is probably too high, yielding overestimates of the uncertainties. With $L = 10^\circ$ the correlation length of the analysis and $\Delta x = \Delta y = 1^\circ$ the resolution of the grid, in our case the numerical value of the inflation factor was $f_{\mathrm{inf}} = 35.45$.

According to Table 2, the global LGM decrease in the gridded SST was (1.7±0.1) °C. The global tropics (taken to be between 30° S and 30° N) cooled on average by (1.2±0.3) °C, but the tropical Atlantic Ocean by about (1.8±0.6) °C. The cooling in the mid- to high-latitudes was around (3.1±0.2) °C in the North Atlantic Ocean and around (1.4±0.3) °C in the South Atlantic Ocean.

3.4 Changes in the meridional differences

The change in the tropical meridional SST difference was calculated as the average SST anomaly between the equator and 30 °N minus the average SST anomaly between 30 °S and the equator (cf. McGee et al., 2014). According to Table 2 and

standard uncertainty propagation, this difference decreased by (0.4±0.6) °C for the global ocean and by (0.4±1.2) °C for the Atlantic Ocean.

In contrast, the meridional SST difference between the mid- to high-latitudes in the North Atlantic Ocean (north of 45° N) and the South Atlantic Ocean (south of 30° S - these two regions were chosen in accordance with Rahmstorf, 1996) increased by (1.7±0.3) °C.

3.5 Zonal-mean changes

The zonal mean changes for the global ocean and the Atlantic, Pacific and Indian oceans are shown in Fig. 4. Changes in the Atlantic Ocean were larger than in the other oceans, and changes in the mid- to high latitudes were larger than in the low latitudes, except for the tropical South Atlantic Ocean, where they reached -4 °C due to the cooling in the coastal and equatorial upwelling regions.

3.6 Data-analysis misfit

The normalized data-analysis misfit was determined as

$$J_{\text{misfit}} = \frac{1}{N_{\text{data}}} \sum_i \frac{\left(T_i^{\text{gridded}} - T_i^{\text{data}}\right)^2}{u_i^2}\,, \tag{5}$$

where N_{data} is the number of data-analysis pairs. The normalized misfit was $J_{\text{misfit}} = 1.5$ with $N_{\text{data}} = 420$ for JAS and $J_{\text{misfit}} = 1.7$ with $N_{\text{data}} = 528$ for JFM, respectively. The geographic distribution of the individual misfits at the data locations is shown in Fig. 5. Values larger than the uncertainty of the original data occur in the coastal and equatorial upwelling regions and near and under the reconstructed sea-ice cover.

3.7 Comparison to other reconstructions

Table 3 lists the recent studies by Annan and Hargreaves (2013), Kurahashi-Nakamura et al. (2017a) and Tierney et al. (2020) and compares them to our study in terms of the data, model(s) and method used. Maps of annual-mean sea-surface temperature anomalies are shown in Fig. 6. According to Table 4, global ocean cooling across the different reconstructions ranged from 1.5 °C to 3.6 °C, while tropical ocean cooling ranged from 0.9 °C to 3.4 °C. For the Atlantic Ocean with better data coverage than the Pacific Ocean, the tropical cooling was between 1.6 °C and 3.7 °C. In all three cases, the lowest value was from CLIMAP Project Members (1981) and the highest from Tierney et al. (2020). All reconstructions show an amplified cooling in the Atlantic Ocean north of 45° N, with the maximum cooling of 7.1 °C given by CLIMAP (1981).

4 Discussion

The main purpose of our study was to demonstrate the applicability of the DIVA method to sparse paleo data and provide a gridded SST reconstuction for the testing of coupled climate models and forcing of AGCMs. We indeed found that the DIVA

method was capable of analyzing data that were much sparser than current oceanographic observations, with a skill that was comparable to variogram analysis and kriging, but thanks to the underlying global finite-element mesh with less complications (such as the introduction of communication masks to avoid the pairing of data points that are unlikely to influence each other in the real ocean, cf. Schäfer-Neth et al., 2005, Fig. 2). Figures 3 and 5 show that when applied to the paleo data the interpolated fields are neither "noisy" nor "patchy", which is an indication that the data points were not overfitted, resulting in a smooth climatology. In addition, our gridded data set of LGM SST anomalies allowed us to evaluate changes in global and regional averages and spatial differences including their uncertainties.

Following Eq. 3, we calculated the uncertainties of the global and regional averages as the product of the simple sum of the diagonal terms of the error covariance matrix and an inflation factor, which probably resulted in overestimates. In fact, DIVA may be used to more accurately estimate the spatial covariances as described by the non-diagonal terms, albeit at a much higher computational cost (Troupin et al., 2012; Beckers et al., 2014; Troupin et al., 2019, Section 4.5; see also Wunsch, 2018). Therefore we decided to use the simplified inflation approach. We obtained a mean change for the global ocean of (-1.7±0.1) °C and a mean change for the tropical ocean between 30° S and 30° N of (-1.2±0.3) °C. As compared to MARGO Project Members (2009, Table 1), these values tend to be smaller by 0.2 °C to 0.3 °C, possibly because the MARGO results are based on block-averaged SST anomalies with an incomplete coverage biased towards the eastern continental margin, while our results are based on complete fields obtained from the DIVA analysis.

Our result of a change in the tropical meridional SST difference by (0.41±0.6) °C reflects a greater cooling in the southern tropics than in the northern tropics, mainly due to changes in the coastal and equatorial upwelling regions. It is consistent with the original MARGO synthesis (cf. MARGO Project Members, 2009, Figs. 3 and 4), but inconsistent with, e.g., McGee et al. (2014) who estimate a change of (-0.14±0.18) °C that indicates a greater cooling in the northern tropics than in the southern tropics. According to McGee et al. (2014, Fig. 3), our result would correspond to a northward shift of the ITCZ by (0.8±1.3)° and a decrease of the cross-equatorial heat transport by (0.31±0.5) PW, while McGee et al. (2014) obtain a southward shift by (-0.29±0.38)° and an increase by (0.11±0.14) PW. Part of the differences may be due to our denser data coverage and that we based our calculation of regional averages on a gridded analysis as opposed to single ocean sediment cores or block averages with incomplete coverage. However, we stress that strictly speaking neither our results nor the results by McGee et al. (2014) are statistically significant, because the inferred changes are smaller than their estimated uncertainties.

In contrast, the increase of the meridional SST difference between the mid- to high-latitudes in the North Atlantic Ocean and the South Atlantic Ocean of (1.7±0.3) °C is statistically significant and by itself would argue for an intensified Atlantic meridional overturning circulation, which is indeed found in some simulations of the LGM ocean circulation (e.g., Kurahashi-Nakamura et al., 2017b). However, this increase may be counteracted by an accompanying decrease of the sea-surface salinity gradient, which may result in an overall decrease of the sea-surface density gradient (e.g., Paul and Schäfer-Neth, 2003). Both the decrease of the tropical meridional SST difference and the increase of the large-scale Atlantic meridional SST difference are also evident from the zonal-mean SST changes in Fig. 4.

The normalized misfits of $J_{\mathrm{misfit}} = 1.5$ for JAS and $J_{\mathrm{misfit}} = 1.7$ for JFM mean that on average the misfit was larger than the uncertainty of the original data by 50 % to 70 %. However, the geographic distribution shows that large misfits were restricted

to certain regions (e.g., subject to large variations due to upwelling or sea-ice cover) and maybe due to deviations between near-by sediment core locations.

We deliberately made use of the separate summer and winter temperature reconstructions based on the faunal and floral transfer function technique. This technique may not provide fully independent seasonally resolved SST reconstructions (cf. Mix et al., 2001; Morey et al., 2005) but partly reflect the seasonal SST structure of the calibration data set (Kucera et al., 2005b), as indicated by the very high correlation ($r \approx 0.94$) between the seasonal reconstructions and the winter and summer SST in the calibration data sets (Kucera et al., 2005b). However, we are confident that some information on the amplitude of the seasonal cycle may still be inferred from microfossil abundances using the faunal and floral transfer function technique as long as both warmth- and cold-loving species are present and no-analog situations are avoided.

As detailed in Table 3, the recent studies by Annan and Hargreaves (2013), Kurahashi-Nakamura et al. (2017b) and Tierney et al. (2020) use different data sets, models and methods. They all involve one or several dynamic models. For example, Kurahashi-Nakamura et al. (2017a) use the method-of-Lagrange-multipliers or "adjoint method" (Wunsch, 1996) in combination with a particular ocean general circulation model (MITgcm). Given its physics and paramaterizations, the resulting field is dynamically consistent with the model, however, it also reflects its structural uncertainty, for example, as evident in the weak cooling or even warming near the eastern boundaries in Fig. 6, coastal upwelling systems cannot be resolved by a coarse-resolution ocean model. On the other hand, it shows a shift in the subtropical front at about 30° latitude in either hemisphere that is not seen in any of the other reconstructions. In contrast, our reconstruction is based on a statistical model, which makes fewer assumptions on how two data points are connected to each other, but it also lacks dynamically consistent constraints. This may explain why our results indicate a slight warming in the tropical Pacific Ocean caused by the interpolation of a few and uncertain data points, in contrast to the dynamic models that induce a cooling comparable to that in the tropical Atlantic Ocean. The reconstruction by Tierney et al. (2020) is based on a different data set that consists of geochemical proxies only and is combined with a particular coupled climate model (iCESM1.2) using an "off-line" data assimilation method. It yields a larger, more homogeneous cooling, except for the high southern latitudes, in which the Pacific sector cools more than the Atlantic sector. When comparing the area-weighted regional anomalies in Table 4, we find that our results on global and tropical ocean cooling are in the range of those that are also based on the MARGO faunal and floral assemblages, but lower than in the reconstruction by Tierney et al. (2020) based on geochemical proxies.

At the level of individual ocean sediment cores, the best resolved alkenone-based SST estimates from the central Pacific Ocean show an SST change between 1.2 °C and 2 °C (Broccoli and Marciniak, Broccoli and Marciniak; Prahl et al., 1989; Lee et al., 2001; de Garidel-Thoron et al., 2007). From a number of studies using Mg/Ca as well as alkenones, Lea (2004) find a tropical cooling at the LGM by 2.8 °C $\pm$ 0.7 °C. Leduc et al. (2017) summarize the results of the Sensitivity of the Tropics (SENSETROP) working group, which after the incorporation of high-quality records and a thorough quality control obtains a cooling of the low latitudes during the LGM of -2.3 °C $\pm$ 0.8 °C and -2.4 °C $\pm$ 0.8°C for alkenone- and Mg/Ca-based SST estimates, respectively. Tierney et al. (2020) obtain a very similar mean tropical cooling of -2.5 °C (-2.8 °C to -2.2 °C, 95 % confidence interval) from the SST proxies on their own. These values are larger than the estimates by CLIMAP, MARGO and

Annan and Hargreaves (2013) by up to a degree, but not as large as the early estimate from corals by Guilderson et al. (1994) of about 5 °C (see also the summary in Manabe and Broccoli, 2020).

A possible reason for the difference between faunal and floral and geochemical proxies is the so-called no-analog problem: There may be assemblages in the fossil record that do not have a counterpart in the modern calibration data set. However, the MARGO project in particular carefully dealt with this problem in a number of ways. For example, Gersonde et al. (2005) discard all samples with no analogs (dissimilarity > 0.25) and when the majority of the samples in the LGM interval has no anlogs, the estimated quality level is downgraded to 3. Kucera et al. (2005b) combine three methods (Artificial Neural Networks – ANN, Revised Analog Method – RAM, Maximum Similarity Technique – SIMMAX) in a multi-technique approach that facilitates a test of the robustness of SST estimates and provides a means to identify potential no-analog conditions or faunas.

Another possible reason are low sedimentation rates, in particular in the tropical Pacific Ocean, but in comparing different proxies, de Garidel-Thoron et al. (2007) find in a well-resolved alkenone record from the western Pacific Warm Pool a cooling by 1 °C to 2°C only, too, which would be consistent with the MARGO results.

While faunal and floral assemblages offer some advantages over geochemical proxies regarding spatial coverage, their potential to provide a seasonal reconstruction and internal consistency, they are not without issues. For example, there are large discrepancies between the SST reconstructions from foraminiferal and dinocyst assemblages in the Nordic Seas (de Vernal et al., 2006). The apparently warm signal recorded by dinocyst assemblages may be due to long-distance lateral transport (de Vernal et al., 2006). Further issues with dinoflagellates are their overwintering in a cyst phase and broad tolerances for temperature (Dale, 2001). Coccolithophores and alkenones are also prone to long-distance lateral transport (Rühlemann and Butzin, 2006), whereas foraminifera-based proxies have the advantage that their signal carriers drop relatively quickly to the sediment (Takahashi and Be, 1984). In addition, using alkenones for SST reconstructions in high latitudes may be problematic because of the low sensitivity of the calibration of alkenones at low temperature (Conte et al., 2006), the possibility of redeposition of old and warm signal carrying alkenones with particulate matter originating from the glaciated continental margins and once more the influence of alkenones transported by currents from warmer areas into the polar regions (e.g., Bendle and Rosell-Melé, 2004; Filippova et al., 2016).

Since foraminiferal assemblages are usually dominated by species adapted to the environment of the overlying water column (Morey et al., 2005), we consider the temperature estimation to be more robust against the expatriation of single shells that can affect proxies measured on monospecific samples. Finally, proxies based on the chemistry of shells of living organisms suffer from the inherent problem that the environmental sensitivity of that organism biases the recording of the proxy (Mix, 1987; Fraile et al., 2009). The transfer function method does not have this problem since it actually uses the environmental sensitivity of the fauna.

From this discussion we conclude that assemblages of living foraminifera faithfully record environmental conditions. However, there are a number of challenges in interpreting the fossil record, in attributing the result to a certain season and water depth and estimating a global cooling from the still sparse and irregularly spaced data set:

1. *Change in seasonality*: Ravelo et al. (1990) demonstrate that in the equatorial Atlantic Ocean faunal assemblages do not respond primarily to SST, but rather to thermocline and seasonality changes. In fact, using a foraminifera model, Fraile

et al. (2009b) show that during the LGM, the maximum production of subtropical as well as high-latitude foraminifera is generally shifted towards a warmer season of the year. For tropical species the change in seasonality did not produce an important temperature bias, because the amplitude of the annual cycle is relatively low.

2. *Change in thermal structure*: Telford et al. (2013) indeed provide evidence that planktonic foraminifera assemblages can be more sensitive to subsurface temperatures than the 10-m SST that they are usually calibrated against, e.g., as in MARGO. They conclude that reconstructions of the 10-m SST are likely to be biased, with the sign and magnitude of the bias varying regionally, but probably causing a warm bias in the tropical North Atlantic. However, foraminifera-based reconstructions for other ocean basins still need to be assessed.

3. *Sampling bias*: The majority of SST estimates comes from the continental margins and exhibits systematic deviations from the open ocean that are related to gyre circulation [cf. Judd et al. (2020) and references therein]. For example, eastern continental margins are dominated by coastal upwelling of cold sub-surface water and radiative cooling and less sensitive to surface cooling and hence are prone to yield a reduced glacial-interglacial contrast. Judd et al. (2020) also point out that data assimilation methods may be helpful in overcoming this spatial bias, provided that the models capture the zonal heterogeneity in temperature due to coastal dynamics.

Taken at face value, and using the same linear relationship by Schneider von Deimling et al. (2006, their Fig. 6) as the MARGO Project Members (2009), our result of a mean change for the tropical Atlantic Ocean of (-2.1±0.7) °C [here for consistency with Schneider von Deimling et al. (2006) taken between 20° S and 20° N] would correspond to an equilibrium climate sensitivity of (1.5±1.0) °C. This is at the low end of the classical range from 1.5 °C to 4.5 °C considered to be likely by Collins et al. (2013, Box 12.2), and it is even lower than the estimate by the MARGO Project Members (2009) of (2.3±1.3) °C. However, these values need to be put in a proper perspective.

On the one hand, our discussion shows that because of changes in seasonality and thermal structure as well as uneven sampling, our estimate of the global and tropical SST decrease based on the MARGO faunal and floral assemblages is likely to biased towards lower values. While at present this is difficult to quantify, the geochemial proxies at the tropical sediment core sites investigated by Lea (2004), Leduc et al. (2017) and Tierney et al. (2020) indeed suggest a cooling of around 2.5 °C, larger by about 0.5 °C to 1 °C. Whether it should be even larger as proposed by Tierney et al. (2020) based on their off-line data assimilation still needs to be independently confirmed. In any case, according to the simple linear relationship by Schneider von Deimling et al. (2006), a larger cooling would also imply a higher equilibrium climate sensitivity.

On the other hand, in view of the recent comprehensive review by Sherwood et al. (2020), estimating the equilibrium climate sensitivity is a very challenging task and simply using a linear relationship derived from a single model does not seem to be an adequate approach. Combining three lines of evidence (observed climate processes, historical climate changes and paleoclimate changes), these authors conclude that the equilibrium climate sensitivity is likely in the slightly narrower range between 2.6 °C and 4.1 °C (at a 66 % level of confidence). One of the two periods that they consider for paleoclimate evidence is the LGM, for which they assume a global surface air temperature decrease of about 3 °C to 7° C with respect to the pre-industrial period

(Sherwood et al., 2020, Section 5.2.1), according to the authors a value inferred from observations at low latitudes (Sherwood et al., 2020, Section 5.2.4).

Based on the reconstruction by Annan and Hargreaves (2013), who apply multiple linear regression to the PMIP2 ensemble of climate models (Braconnot et al., 2007), a decrease in sea-surface temperature in the tropical Atlantic Ocean of 1.5 °C corresponds to a decrease of global surface air temperature by (4.0 ± 0.8) °C (95 % confidence interval). Hence we expect the tropical cooling between 1.0 °C and 1.5 °C in our and the original MARGO reconstruction to be consistent with a decrease of global surface air temperature by about 3°C, which in the analysis by Sherwood et al. (2020) would contribute to their lower limit on the equilibrium climate sensitivity of 2.6 °C, while a tropical cooling of around 2.5 °C or larger as inferred from reconstructions based on geochemical proxies would place the equilibrium climate sensitivity more in the middle of their range.

5 Conclusions

In summary:

- We demonstrated that the Data-Interpolating Variational Analysis (DIVA Troupin et al., 2012) method can be applied to irregularly spaced data that are much sparser than current oceanographic observations, at a computational cost that is orders of magnitude lower than assimilationg the data in a coupled climate or ocean model.
- Consequently, using DIVA, we derived an internally consistent climatology of the monthly SST and sea-ice extent during the LGM on a global 1° × 1° grid from MARGO microfossil assemblages (Kucera et al., 2005a) and a number of sea-ice reconstructions.
- Based on this gridded climatology, we confirmed that the longitudinal and meridional SST differences were likely to be greater than today.
- Using the uncertainty estimate provided by DIVA as a weight, we calculated global and regional averages, quantified the meridional SST differences, estimated the respective uncertainties, and, for example, obtained a cooling of the global ocean by (1.7±0.1) °C and of the tropical ocean by (-1.2±0.3) °C.
- From a review of processes that affect faunal and floral assemblages we concluded that they are faithful recorders of the actual environmental conditions, but that there are a number of challenges in interpreting their fossil record, especially in attributing the local sedimentary imprint to a particular season and water depth.
- Hence anticipated changes in seasonality and thermal structure and a spatial sampling bias, as well as a comparison to geochemical proxies at comparable sites, let us conjecture that results on global and tropical cooling based on faunal and floral assemblages are likely to be biased towards lower values by at least 0.5 °C to 1 °C.

– This implies that estimates of equilibrium climate sensitivity derived from estimates global and tropical cooling based on faunal and floral assemblages and taken at face value tend to be on the low side, too, while estimates based on geochemical proxies would place it more in the middle of the range given in the recent review by Sherwood et al. (2020).

6 Outlook

We expect the Glacial Ocean Map (GLOMAP), in terms of the gridded field and error estimate provided by DIVA, to prove useful in several ways, for example, in evaluating coupled climate models and forcing AGCMs in simulations of the climate of the LGM, or in first smoothing and spreading the original sparse data before using it in constraining an inverse model (cf. Marchal and Curry, 2008). Regarding the first application, we plan to use water isotopes as a tool to compare the performance of different AGCMs, using our gridded GLOMAP SST climatology as a common boundary condition. This way we can on the one hand avoid the propagation of the simulated SST bias in coupled climate models, and on the other hand we can isolate the impact of the ocean feedback on the simulated distributions of water isotopes over land, ice and ocean (e.g., Werner et al., 2018). We also plan to extend our method to δ^{18}O from fossil calcite shells of planktonic foraminifera. A combined reconstruction of SST, sea ice coverage and the inferred δ^{18}O of sea water may be used for an enhanced evaluation of coupled climate models. Regarding future additions to the MARGO database, we hope for an improved coverage of the interior oceans, particularly the tropical Pacific Ocean and the Northwestern Atlantic Ocean. Our application of the DIVA may be further refined by, for example, including advection by surface currents. Improving the attribution of fossil faunal and floral assemblages to certain season or water depths would, however, require a more complex approach, for example, by combining a coupled climate model with a planktonic foraminifera model such as PLAFOM in Kretschmer et al. (2018).

Data availability. The GLOMAP gridded climatology of monthly LGM SST anomalies (including their uncertainties) and monthly estimates of LGM sea-ice extent will be made available through PANGAEA (https://www.pangaea.de). It may be updated when new reconstructions become available.

Competing interests. The authors declare that they have no conflict of interest.

Acknowledgements. This work was supported by the German Federal Ministry of Education and Research (BMBF) as a Research for Sustainability initiative (FONA) through the PalMod project (FKZ: 01LP1511D) as well as by the DFG Research Center/Center of Excellence MARUM – “The Ocean in the Earth System”.

References

Abelmann, A. and Gersonde, R.: Biosiliceous particle flux in the Southern Ocean, Marine Chemistry, 35, 503–536, 1991.

Annan, J. D. and Hargreaves, J. C.: A new global reconstruction of temperature changes at the Last Glacial Maximum, Climate of the Past, 9, 367–376, https://doi.org/10.5194/cp-9-367-2013, 2013.

Beckers, J.-M., Barth, A., Troupin, C., and Alvera-Azcárate, A.: Approximate and Efficient Methods to Assess Error Fields in Spatial Gridding with Data Interpolating Variational Analysis (DIVA), Journal of Atmospheric and Oceanic Technology, 31, 515–530, https://doi.org/10.1175/JTECH-D-13-00130.1, 2014.

Bendle, J. and Rosell-Melé, A.: Distributions of UK37 and UK´37 in the surface waters and sediments of the Nordic Seas: Implications for paleoceanography, Geochemistry, Geophysics, Geosystems, 5, https://doi.org/10.1029/2004GC000741, 2004.

Braconnot, P., Otto-Bliesner, B., Harrison, S., Joussaume, S., Peterchmitt, J.-Y., Abe-Ouchi, A., Crucifix, M., Driesschaert, E., Fichefet, T., Hewitt, C. D., Kageyama, M., Kitoh, A., Laine, A., Loutre, M.-F., Marti, O., Merkel, U., Ramstein, G., Valdes, P., Weber, S. L., Yu, Y., and Zhao, Y.: Results of PMIP2 coupled simulations of the Mid-Holocene and Last Glacial Maximum -Part 1: experiments and large-scale features, Climate of the Past, 3, 261–277, https://doi.org/10.5194/cp-3-261-2007, 2007.

Briggs, R. D., Pollard, D., and Tarasov, L.: A data-constrained large ensemble analysis of Antarctic evolution since the Eemian, Quaternary Science Reviews, 103, 91–115, https://doi.org/10.1016/j.quascirev.2014.09.003, 2014.

Broccoli, A. J. and Marciniak, E. P.: Comparing simulated glacial climate and paleodata: A reexamination, Paleoceanography, 11, 3–14, 1996.

CLIMAP Project Members: The Surface of the Ice-Age Earth, Science, 191, 1131, https://doi.org/10.1126/science.191.4232.1131, 1976.

CLIMAP Project Members: Seasonal reconstructions of the Earth's surface at the Last Glacial Maximum, Geological Society of America, Map and Chart Series, MC-36, 1–18, 1981.

Collins, M., Knutti, R., Arblaster, J., Dufresne, J.-L., Fichefet, T., Friedlingstein, P., Gao, X., Gutowski, W., Johns, T., Krinner, G., Shongwe, M., Tebaldi, C., Weaver, A., and Wehner, M.: Long-term Climate Change: Projections, Commitments and Irreversibility, in: Climate Change 2013: The Physical Science Basis. Contribution of Working Group I to the Fifth Assessment Report of the Intergovernmental Panel on Climate Change, edited by Stocker, T., Qin, D., Plattner, G.-K., Tignor, M., Allen, S., Boschung, J., Nauels, A., Xia, Y., Bex, V., and Midgley, P., pp. 1029–1136, Cambridge University Press, 2013.

Conte, M. H., Sicre, M.-A., Rühlemann, C., Weber, J. C., Schulte, S., Schulz-Bull, D., and Blanz, T.: Global temperature calibration of the alkenone unsaturation index (UK′37) in surface waters and comparison with surface sediments, Geochemistry, Geophysics, Geosystems, 7, Q02 005, https://doi.org/10.1029/2005GC001054, 2006.

Dale, B.: The sedimentary record of dinoflagellate cysts: Looking back into the future of phytoplankton blooms, Scientia Marina, 65, 257–272, 2001.

de Garidel-Thoron, T., Rosenthal, Y., Beaufort, L., Bard, E., Sonzogni, C., and Mix, A. C.: A multiproxy assessment of the western equatorial Pacific hydrography during the last 30 kyr, Paleoceanography, 22, https://doi.org/10.1029/2006PA001269, 2007.

de Vernal, A., Eynaud, F., Henry, M., Hillaire-Marcel, C., Londeix, L., Mangin, S., Mathiessen, J., Marret, F., Radi, T., Rochon, A., Solignac, S., and Turon, J.-L.: Reconstruction of sea-surface conditions at middle to high latitudes of the Northern Hemisphere during the Last Glacial Maximum (LGM) based on dinoflagellate cyst assemblages, Quaternary Science Reviews, 24, 897–924, https://doi.org/10.1016/j.quascirev.2004.06.014, 2005.

de Vernal, A., Rosell-Melé, A., Kucera, M., Hillaire-Marcel, C., Eynaud, F., Weinelt, M., Dokken, T., and Kageyama, M.: Comparing proxies for the reconstruction of LGM sea-surface conditions in the northern North Atlantic, Quaternary Science Reviews, 25, 2820–2834, https://doi.org/10.1016/j.quascirev.2006.06.006, 2006.

Deutsch, C. V. and Journel, A. G.: GSLIB, Geostatistical Software Library and User's Guide, Oxford University Press, New York, Oxford, 1992.

Eisenman, I.: Geographic muting of changes in the Arctic sea ice cover, Geophysical Research Letters, 37, https://doi.org/10.1029/2010GL043741, 2010.

Filippova, A., Kienast, M., Frank, M., and Schneider, R. R.: Alkenone paleothermometry in the North Atlantic: A review and synthesis of surface sediment data and calibrations, Geochemistry, Geophysics, Geosystems, 17, 1370–1382, https://doi.org/10.1002/2015GC006106, 2016.

Fischer, G., Gersonde, R., and Wefer, G.: Organic carbon, biogenic silica and diatom fluxes in the marginal winter sea ice zone and in the Polar Front Region in the Southern Ocean (Atlantic sector): interannual variation and changes in composition, Deep-Sea Research II, 49, 1721–1745, https://doi.org/10.1016/S0967-0645(02)00009-7, 2002.

Fraile, I., Mulitza, S., and Schulz, M.: Modeling planktonic foraminiferal seasonality: Implications for sea-surface temperature reconstructions, Marine Micropaleontology, 72, 1–9, https://doi.org/10.1016/j.marmicro.2009.01.003, 2009.

Fraile, I., Schulz, M., Mulitza, S., Merkel, U., Prange, M., and Paul, A.: Modeling the seasonal distribution of planktonic foraminifera during the Last Glacial Maximum, Paleoceanography, 24, PA2216, doi:10.1029/2008PA001 686, 2009b.

Gersonde, R. and Zielinski, U.: The reconstruction of late Quaternary Antarctic sea-ice distribution –the use of diatoms as proxies for sea-ice, Paleogeography, Paleoclimatology and Paleoecology, 162, 263–286, https://doi.org/10.1016/S0031-0182(00)00131-0, 2000.

Gersonde, R., Crosta, X., Abelmann, A., and Armand, L.: Sea-surface temperature and sea ice distribution of the Southern Ocean at the EPILOG Last Glacial Maximum – a circum-Antarctic view based on siliceous microfossil records, Quaternary Science Reviews, 24, 869–896, https://doi.org/doi:10.1016/j.quascirev.2004.07.015, 2005.

Giraud, X. and Paul, A.: Interpretation of the paleo–primary production record in the NW African coastal upwelling system as potentially biased by sea level change, Paleoceanography, 25, https://doi.org/10.1029/2009PA001795, 2010.

Guilderson, T. P., Fairbanks, R. G., and Rubenstone, J. L.: Tropical Temperature Variations Since 20,000 Years Ago: Modulating Interhemispheric Climate Change, Science, 263, 663–665, https://doi.org/10.1126/science.263.5147.663, 1994.

Jansen, E., Overpeck, J., Briffa, K., Duplessy, J.-C., Joos, F., Masson-Delmotte, V., Olago, D., Otto-Bliesner, B., Peltier, W., Rahmstorf, S., Ramesh, R., Raynaud, D., Rind, D., Solomina, O., Villalba, R., and Zhang, D.: Palaeoclimate, in: Climate Change 2007: The Physical Science Basis. Contribution of Working Group I to the Fourth Assessment Report of the Intergovernmental Panel on Climate Change, edited by Solomon, S., Qin, D., Manning, M., Chen, Z., Marquis, M., Averyt, K., Tignor, M., and Miller, H., pp. 447–451, Cambridge University Press, Cambridge, United Kingdom and New York, NY, USA, 2007.

Judd, E. J., , Bhattacharya, T., and Ivany, L. C.: A Dynamical Framework for Interpreting Ancient SeaSurface Temperature, Geophysical Research Letters, 47, e2020GL089 044, https://doi.org/10.1029/2020GL089044, 2020.

Kageyama, M., Albani, S., Braconnot, P., Harrison, S. P., Hopcroft, P. O., Ivanovic, R. F., Lambert, F., Marti, O., Peltier, W. R., Peterschmitt, J.-Y., Roche, D. M., Tarasov, L., Zhang, X., Brady, E. C., Haywood, A. M., LeGrande, A. N., Lunt, D. J., Mahowald, N. M., Mikolajewicz, U., Nisancioglu, K. H., Otto-Bliesner, B. L., Renssen, H., Tomas, R. A., Zhang, Q., Abe-Ouchi, A., Bartlein, P. J., Cao, J., Li, Q., Lohmann, G., Ohgaito, R., Shi, X., Volodin, E., Yoshida, K., Zhang, X., and Zheng, W.: The PMIP4 contribution to CMIP6 – Part 4: Sci-

entific objectives and experimental design of the PMIP4-CMIP6 Last Glacial Maximum experiments and PMIP4 sensitivity experiments, Geoscientific Model Development, 10, 4035–4055, https://doi.org/10.5194/gmd-10-4035-2017, 2017.

Kretschmer, K., Jonkers, L., Kucera, M., and Schulz, M.: Modeling seasonal and vertical habitats of planktonic foraminifera on a global scale, Biogeosciences, 15, 4405–4429, https://doi.org/10.5194/bg-15-4405-2018, 2018.

Kucera, M., Rosell-Melé, A., Schneider, R., Waelbroeck, C., and Weinelt, M.: Multiproxy approach for the reconstruction of the glacial ocean surface (MARGO), Quaternary Science Reviews, 24, 813–819, 2005a.

Kucera, M., Weinelt, M., Kiefer, T., Pflaumann, U., Hayes, A., Weinelt, M., Chen, M.-T., Mix, A. C., Barrows, T. T., Cortijo, E., Duprat, J., Juggins, S., and Waelbroeck, C.: Reconstruction of sea-surface temperatures from assemblages of planktonic foraminifera: Multi-technique approach based on geographically constrained calibration data sets and its application to glacial Atlantic and Pacific Oceans, Quaternary Science Reviews, 24, 951–998, https://doi.org/doi:10.1016/j.quascirev.2004.07.014, 2005b.

Kurahashi-Nakamura, T., Paul, A., and Losch, M.: Dynamical reconstruction of the global ocean state during the Last Glacial Maximum, Paleoceanography, 32, 326–350, https://doi.org/10.1002/2016PA003001, 2017a.

Kurahashi-Nakamura, T., Paul, A., and Losch, M.: Dynamical reconstruction of the global ocean state during the Last Glacial Maximum, Paleoceanography, 32, 326–350, https://doi.org/10.1002/2016PA003001, 2017b.

Lea, D. W.: The 100,000-yr Cycle in Tropical SST, Greenhouse Forcing, and Climate Sensitivity, Journal of Climate, 17, 2170–2179, 2004.

Leduc, G., de Garidel-Thoron, T., Kaiser, J., Bolton, C., and Contoux, C.: Databases for sea surface paleotemperature based on geochemical proxies from marine sediments: implications for model-data comparisons, Quaternaire, 28, 201–216, https://doi.org/10.4000/quaternaire.8034, http://quaternaire.revues.org/8034, 2017.

Lee, K. E., Slowey, N. C., and Herbert, T. D.: Glacial sea surface temperatures in the subtropical North Pacific: A comparison of $U^{k'}_{37}$, $\delta^{18}O$, and foraminiferal assemblage temperature estimates, Paleoceanography, 16, https://doi.org/10.1029/1999PA000493, 2001.

Levitus, S.: Climatological atlas of the World Ocean, NOAA Prof. Paper No. 13, p. 173 pp., 1982.

Manabe, S. and Broccoli, A. J.: Beyond Global Warming, Princeton University Press, https://doi.org/10.1515/9780691185163, 2020.

Marchal, O. and Curry, W. B.: On the Abyssal Circulation in the Glacial Atlantic, Journal of Physical Oceanography, 38, 2014–2037, https://doi.org/doi: 10.1175/2008JPO3895.1, 2008.

MARGO Project Members: Constraints on the magnitude and patterns of ocean cooling at the Last Glacial Maximum, Nature Geoscience, 2, 127–132, https://doi.org/doi:10.1039/NGEO411, 2009.

Masson-Delmotte, V., Schulz, M., Abe-Ouchi, A., Beer, J., Ganopolski, A., González Rouco, J., Jansen, E., Lambeck, K., Luterbacher, J., Naish, T., Osborn, T., Otto-Bliesner, B., Quinn, T., Ramesh, R., Rojas, M., Shao, X., and Timmermann, A.: Information from Paleoclimate Archives, in: Climate Change 2013: The Physical Science Basis. Contribution of Working Group I to the Fifth Assessment Report of the Intergovernmental Panel on Climate Change, edited by Stocker, T., Qin, D., Plattner, G.-K., Tignor, M., Allen, S., Boschung, J., Nauels, A., Xia, Y., Bex, V., and Midgley, P., pp. 383–464, Cambridge University Press, Cambridge, United Kingdom and New York, NY, USA, 2013.

McGee, D., Donohoe, A., Marshall, J., and Ferreira, D.: Changes in ITCZ location and cross-equatorial heat transport at the Last Glacial Maximum, Heinrich Stadial 1, and the mid-Holocene, Earth and Planetary Science Letters, 390, 69–79, https://doi.org/10.1016/j.epsl.2013.12.043, 2014.

Méheust, M., Ruediger Stein, R., Fahl, K., Max, L., and Riethdorf, J. R.: High-resolution IP25-based reconstruction of sea-ice variability in the western North Pacific and Bering Sea during the past 18,000 years, Geo-Marine Letters, 36, 101–111, https://doi.org/10.1007/s00367-015-0432-4, 2016.

Méheust, M., Ruediger Stein, R., Fahl, K., and Gersonde, R.: Sea-ice variability in the subarctic North Pacific and adjacent Bering Sea during the past 25 ka: new insights from IP25 and $U^{k'}_{37}$ proxy records, Arktos, 4, https://doi.org/10.1007/s41063-018-0043-1, 2018.

Mix, A. C.: The oxygen-isotope record of glaciation, in: North America and adjacent oceans during the last deglaciation, edited by Ruddiman, W. F. and Wright, Jr., H. E., vol. K-3 of *The Geology of North America*, Geological Society of America, Boulder, Colorado, https://doi.org/10.1130/DNAG-GNA-K3.111, 1987.

Mix, A. C., Bard, E., and Schneider, R.: Environmental processes of the ice age: Land, oceans, glaciers (EPILOG), Quaternary Science Reviews, 20, 627–658, 2001.

Morey, A. E., Mix, A. C., and Pisias, N. G.: Planktonic foraminiferal assemblages preserved in surface sediments correspond to multiple environmental variables, Quaternary Science Reviews, 24, 925–950, https://doi.org/10.1016/j.quascirev.2003.09.011, 2005.

Paul, A. and Schäfer-Neth, C.: Modeling the water masses of the Atlantic Ocean at the Last Glacial Maximum, Paleoceanography, 18, doi:10.1029/2002PA000 783, 2003.

Pflaumann, U., Sarnthein, M., Chapman, M., Funnel, B., Huels, M., Kiefer, T., Maslin, M., Schulz, H., Swallow, J., van Kreveld, S., Vautravers, M., Vogelsang, E., and Weinelt, M.: The Glacial North Atlantic: Sea-surface conditions reconstructed by GLAMAP-2000, Paleoceanography, 18, doi:10.1029/2002PA00 774, 2003.

PMIP: Paleoclimate Modelling Intercomparison Project, http://www-pcmdi.llnl.gov/pmip/newsletters/newsletter02.html, Tech. rep., 1993.

Prahl, F. G., Muehlhausen, L. A., and Lyle, M.: An organic geochemical assessment of oceanographic conditions at Manop Site C over the past 26,000 years, Paleoceanography, 4, 495–510, https://doi.org/10.1029/PA004i005p00495, 1989.

Rahmstorf, S.: On the freshwater forcing and transport of the North Atlantic thermohaline circulation, Climate Dynamics, 12, 799–811, 1996.

Ravelo, A. C., Fairbanks, R. G., and Philander, S. G. H.: Reconstructing tropical Atlantic hydrography using planktonic foraminifera and an ocean model, Paleoceanography, 5, 409–431, https://doi.org/DOI: 10.1029/PA005i003p00409, 1990.

Roche, D. M., Crosta, X., and Renssen, H.: Evaluating Southern Ocean sea-ice for the Last Glacial Maximum and pre-industrial climates: PMIP-2 models and data evidence, Quaternary Science Reviews, 56, 99–106, https://doi.org/10.1016/j.quascirev.2012.09.020, 2012.

Rühlemann, C. and Butzin, M.: Alkenone temperature anomalies in the Brazil-Malvinas Confluence area caused by lateral advection of suspended particulate material, Geochemistry, Geophysics, Geosystems, 7, Q10 015, https://doi.org/10.1029/2006GC001251, 2006.

Sarnthein, M., Gersonde, R., Niebler, S., Pflaumann, U., Spielhagen, R., Thiede, J., Wefer, G., and Weinelt, M.: Overview of Glacial Atlantic Ocean Mapping (GLAMAP 2000), Paleoceanography, 18, doi:10.1029/2002PA00 769, 2003a.

Sarnthein, M., Pflaumann, U., and Weinelt, M.: Past extent of sea ice in the northern North Atlantic inferred from foraminiferal paleotemperature estimates, Paleoceanography, 18, https://doi.org/10.1029/2002PA00771, 2003b.

Schäfer-Neth, C. and Paul, A.: The Atlantic Ocean at the Last Glacial Maximum: 1. Objective mapping of the GLAMAP sea-surface conditions, in: The South Atlantic in the Late Quaternary: Reconstruction of Material Budgets and Current Systems, edited by Wefer, G., Mulitza, S., and Ratmeyer, V., pp. 531–548, Springer-Verlag, Berlin, Heidelberg, 2004.

Schäfer-Neth, C., Paul, A., and Mulitza, S.: Perspectives on mapping the MARGO reconstructions by variogram analysis/kriging and objective analysis, Quaternary Science Reviews, 23, 1083–1093, doi:10.1016/j.quascirev.2004.06.017, 2005.

Schneider von Deimling, T., Held, H., Ganopolski, A., and Rahmstorf, S.: Climate sensitivity estimated from ensemble simulations of glacial climate, Climate Dynamics, 27, 149–163, doi:10.1007/s00 382–006–0126–8, 2006.

Sherwood, S., Webb, M. J., Annan, J. D., Armour, K. C., Forster, P. M., Hargreaves, J. C., Hegerl, G., Klein, S. A., Marvel, K. D., Rohling, E. J., Watanabe, M., Andrews, T., Braconnot, P., Bretherton, C. S., Foster, G. L., Hausfather, Z., Heydt, A. S. v. d., Knutti, R., Mauritsen,

T., Norris, J. R., Proistosescu, C., Rugenstein, M., Schmidt, G. A., Tokarska, K. B., and Zelinka, M. D.: An assessment of Earth's climate sensitivity using multiple lines of evidence, Reviews of Geophysics, p. e2019RG000678, https://doi.org/10.1029/2019RG000678, 2020.

Takahashi, K. and Be, A. W. H.: Planktonic foraminifera: factors controlling sinking speeds, Deep Sea Research Part A. Oceanographic Research Papers, 31, 1477–1500, https://doi.org/10.1016/0198-0149(84)90083-9, 1984.

Tarasov, L., Dyke, A. S., Neal, R. M., and Peltier, W. R.: A data-calibrated distribution of deglacial chronologies for the North American ice complex from glaciological modeling, EPSL, 315-316, 30–40, https://doi.org/10.1016/j.epsl.2011.09.010, 2012.

Telford, R. J., Li, C., and Kucera, M.: Mismatch between the depth habitat of planktonic foraminifera and the calibration depth of SST transfer functions may bias reconstructions, Climate of the Past, 9, 859–870, https://doi.org/10.5194/cp-9-859-2013, 2013.

Tierney, J. E., Zhu, J., King, J., Malevich, S. B., Hakim, G. J., and Poulsen, C. J.: Glacial cooling and climate sensitivity revisited, Nature, 584, 569–573, https://doi.org/10.1038/s41586-020-2617-x, 2020.

Troupin, C., Barth, A., Sirjacobs, D., Ouberdous, M., Brankart, J.-M., Brasseur, P., Rixen, M., Alvera-Azcárate, A., Belounis, M., Capet, A., Lenartz, F., Toussaint, M.-E., and Beckers, J.-M.: Generation of analysis and consistent error fields using the Data Interpolating Variational Analysis (DIVA), Ocean Modelling, 52-53, 90–101, https://doi.org/10.1016/j.ocemod.2012.05.002, http://modb.oce.ulg.ac.be, 2012.

Troupin, C., Watelet, S., Ouberdous, M., Sirjacobs, D., Alvera-Azcárate, A., Barth, A., Toussaint, M.-E., and Beckers, J.-M.: Data Interpolating Variational Analysis User Guide, Tech. rep., GeoHydrodynamics and Environment Research (GHER), Departement of Astrophysics, Geophysics and Oceanography, University of Liège, http://modb.oce.ulg.ac.be, 2019.

Tyberghein, L., Verbruggen, H., Pauly, K., Troupin, C., Mineur, F., and De Clerck, O.: Bio-ORACLE: a global environmental dataset for marine species distribution modelling, Global Ecology and Biogeography, 21, 272–281, https://doi.org/10.1111/j.1466-8238.2011.00656.x, 2012.

Werner, M., Jouzel, J., Masson-Delmotte, V., and Lohmann, G.: Reconciling glacial Antarctic water stable isotopes with ice sheet topography and the isotopic paleothermometer, Nature Communications, 9, 3537, https://doi.org/doi:10.1038/s41467-018-05430-y, 2018.

WOA: World Ocean Atlas 1998, Tech. rep., National Oceanographic Data Center, Silver Spring, Maryland, 1998.

Wunsch, C.: The Ocean Circulation Inverse Problem, Cambridge University Press, New York, 1996.

Wunsch, C.: Towards determining uncertainties in global oceanic mean values of heat, salt, and surface elevation, Tellus A: Dynamic Meteorology and Oceanography, 70, 1–14, https://doi.org/10.1080/16000870.2018.1471911, 2018.

Xiao, X., Stein, R., and Fahl, K.: MIS 3 to MIS 1 temporal and LGM spatial variability in Arctic Ocean sea ice cover: Reconstruction from biomarkers, Paleoceanography, 30, 969–983, https://doi.org/10.1002/2015PA002814, 2015.

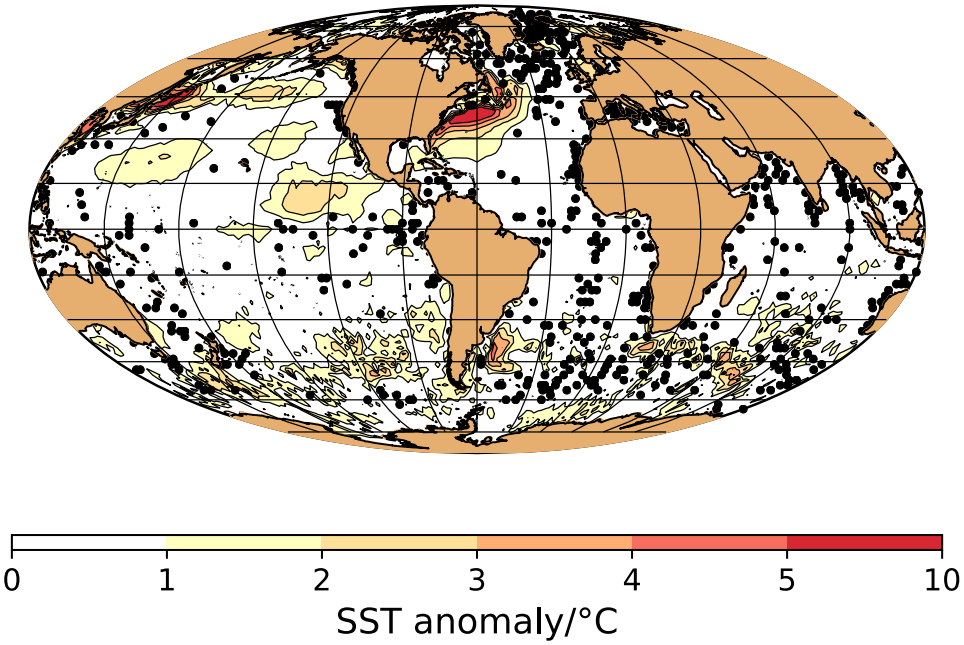

Figure 1. Absolute difference between the analyzed (using Diva) and unanalyzed annual-mean sea-surface temperature (contour lines) and MARGO core locations (black circles).

Ocean	DIVA	Kriging	Levitus
Atlantic	1.33	1.29	1.40
Pacific	1.16 (1.11)	1.19 (1.15)	1.75
Indian	0.73	0.93	1.04
Arctic	1.30	3.52 (1.69)	1.84
Global	1.16 (1.14)	1.22 (1.15)	1.56

Table 1. Root-mean square annual-mean SST differences between the interpolated and observed fields at all WOA (1998) unanalyzed data locations, binned into 2° longitude/latitude squares. Differences in parentheses arise if all SST values below -1.8° C (taken as the freezing point) are set to this value in the analyzed field.

Table 2. Global and regional averages and meridional differences of SST anomalies (LGM - modern) based on data gridded with DIVA and weighted by their uncertainties.

GLOMAP regional averages, meridional differences and uncertainties		
Region	Average	Uncertainty
Global ocean	-1.7	0.1
Global tropical ocean (30° S - 30° N)	-1.2	0.3
Northern tropical ocean (0° - 30° N)	-0.9	0.4
Southern tropical ocean (30° S - 0°)	-1.4	0.4
Tropical meridional difference (north - south)	0.4	0.6
Tropical Atlantic Ocean (30° S - 30° N)	-1.8	0.6
Tropical Atlantic Ocean (20° S - 20° N)	-2.1	0.7
Northern Tropical Atlantic Ocean (0° - 30° N)	-1.6	0.8
Southern Tropical Atlantic Ocean (30° S - 0°)	-2.0	0.8
Tropical Atlantic meridional difference	0.4	1.2
Northern North Atlantic Ocean (> 45° N)	-3.1	0.2
Southern South Atlantic Ocean (< -30° S)	-1.4	0.3
Atlantic meridional difference (north - south)	-1.7	0.3

All temperature anomalies and uncertainties in units of °C

Study	LGM Data	Model(s)	Method
Annan and Hargreaves (2013)	global annual-mean SST (MARGO, 2009) and SAT (Bartlein et al., 2011; Shakun et al., 2012)	PMIP2 ($\approx 1^\circ$ to $\approx 3^\circ$)	multiple linear regression
Kurahashi-Nakamura et al. (2017b)	global annual-mean SST (MARGO, 2009), Atlantic benthic δ^{18}O (Marchal and Curry, 2008) and δ^{13}C (Hesse et al., 2011)	MITgcm ($\approx 3^\circ$)	method-of-Lagrange-multipliers/adjo
Tierney et al. (2020)	global annual-mean SST, various geochemical reconstructions ($U^{K'}_{37}$, TEX_{86}, Mg/Ca, δ^{18}O)	iCESM1.2 ($\approx 1^\circ$)	off-line data assimilation
GLOMAP (this study)	global seasonal SST (MARGO, 2009, faunal and floral assemblages), various sea-ice reconstructions	statistical ($\approx 1^\circ$)	variational inverse method (DIVA)

Table 3. Comparison of global gridded climatologies of the ocean surface during the LGM. With respect to the models employed, the approximate horizontal grid resolution is given in brackets. For more details, see the respective study.

Region	CLIMAP	GLAMAP	AH2013	K2017	T2020	GLOMAP
Global Ocean	-1.5	-1.8	-2.1	-2.0	-3.6	-1.7
Global tropical ocean (20° S - 20° N)	-0.9	-1.2	-1.5	-2.1	-3.4	-1.0
Northern tropical ocean (0° - 20° N)	-1.1	-1.3	-1.6	-2.3	-3.4	-0.8
Southern tropical ocean (20° S - 0°)	-0.7	-1.1	-1.4	-1.8	-3.5	-1.2
Tropical Atlantic Ocean (20° S - 20° N)	-1.6	-2.8	-2.1	-2.4	-3.7	-2.1
Northern Tropical Atlantic Ocean	-1.6	-2.5	-1.9	-3.0	-3.7	-1.6
Southern Tropical Atlantic Ocean	-1.5	-3.2	-2.2	-1.7	-3.7	-2.6
Northern North Atlantic Ocean (> 45° N)	-7.1	-5.8	-3.1	-3.3	-4.8	-5.4
Southern South Atlantic Ocean (< -30° S)	-1.9	-2.4	-2.4	-2.6	-2.2	-2.5

Table 4. Comparison of global gridded climatologies of the ocean surface during the LGM in terms of the area-weighted regional anomalies of the annual-mean SST (CLIMAP = CLIMAP Project Members (1981), GLAMAP = Sarnthein et al. (2003a), AH2013 = Annan and Hargreaves (2013), K2017 = Kurahashi-Nakamura et al. (2017b), T2020 = Tierney et al. (2020) and GLOMAP = this study).

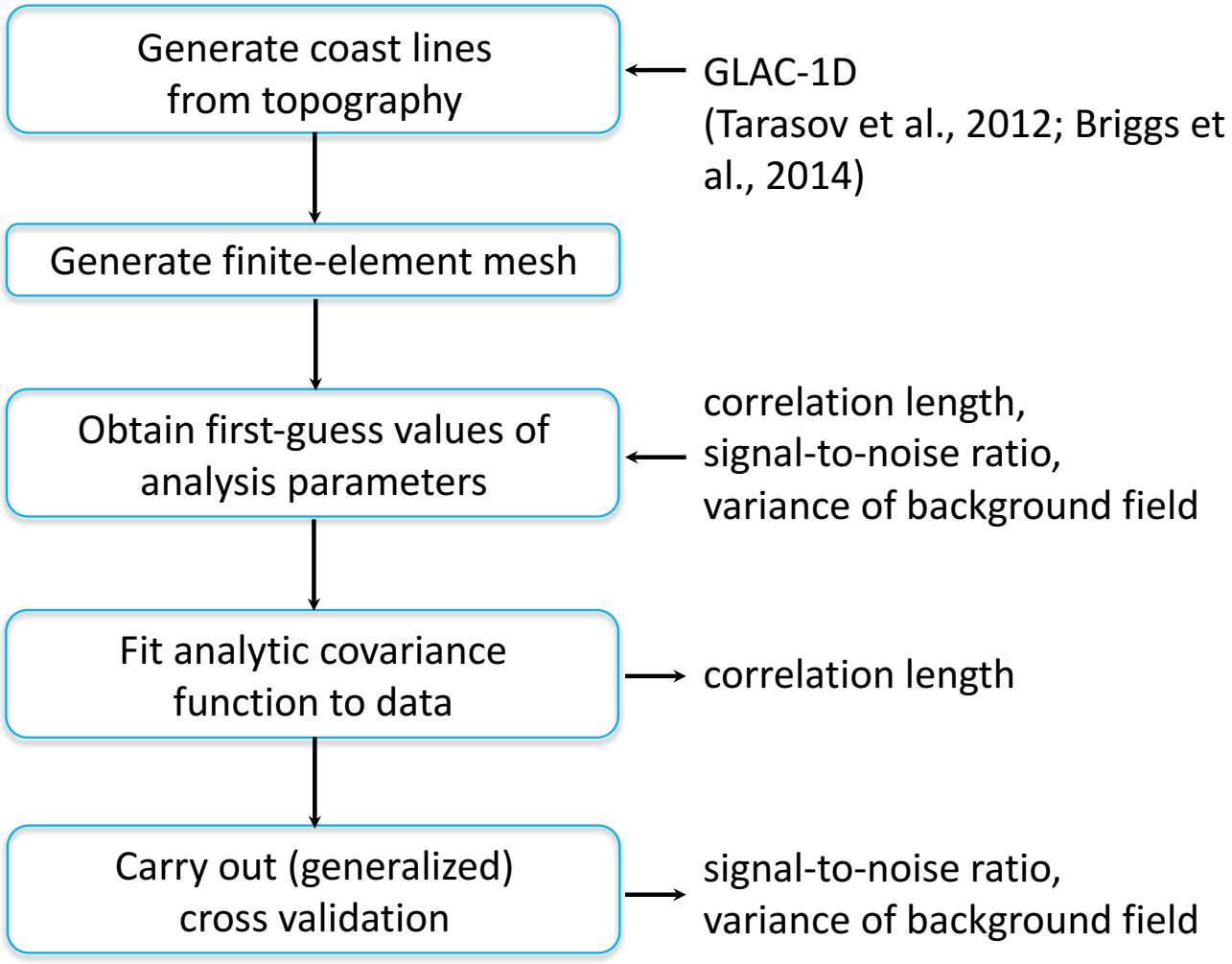

Figure 2. General workflow of DIVA (Data-Interpolating Variational Analysis, Troupin et al.,2012).

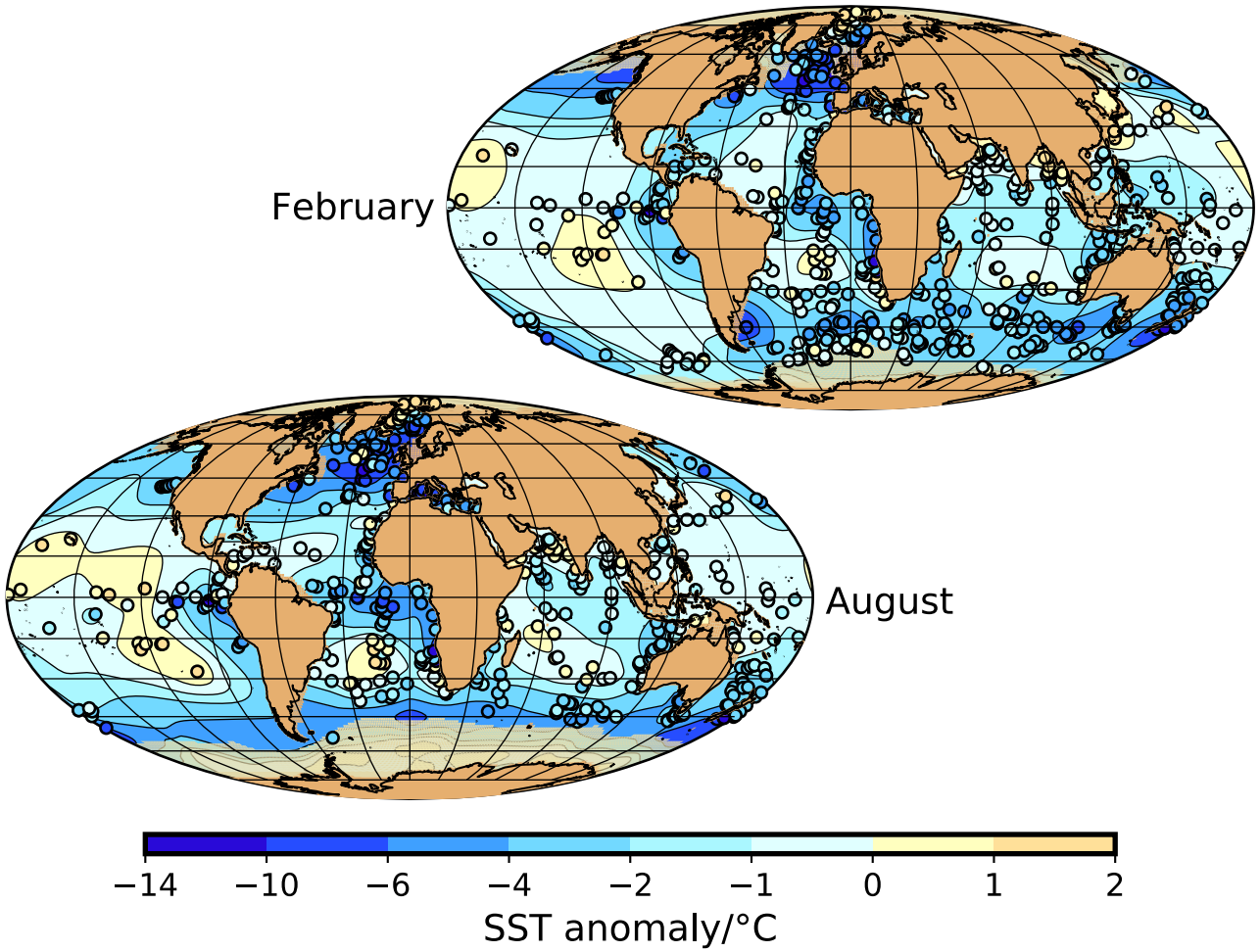

Figure 3. Analyzed LGM SST anomalies for February and August (contour map) and data values (colored circles). The anomalies are relative to WOA (1998). The yellow-brownish areas close to Antarctica and in the Arctic indicate the LGM sea-ice masks based on the selected LGM sea-ice reconstructions.

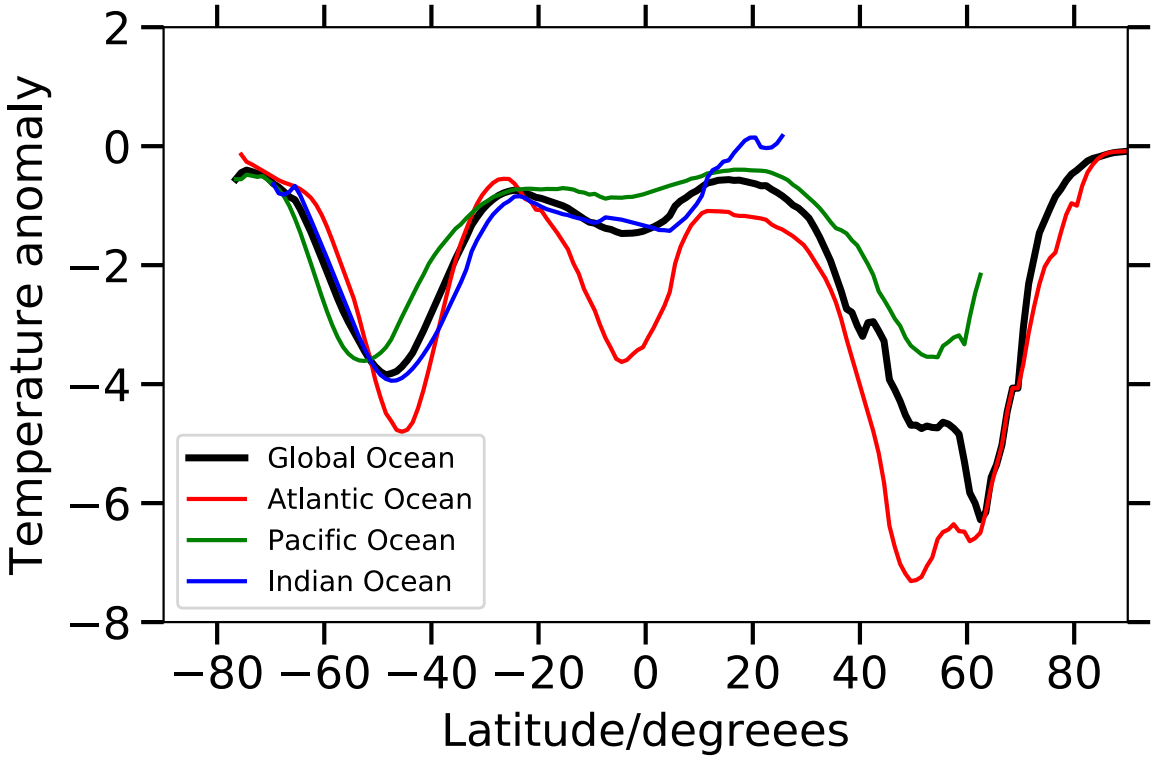

Figure 4. Zonally-averaged annual-mean SST anomalies for the global ocean, Atlantic Ocean, Pacific Ocean and Indian Ocean.

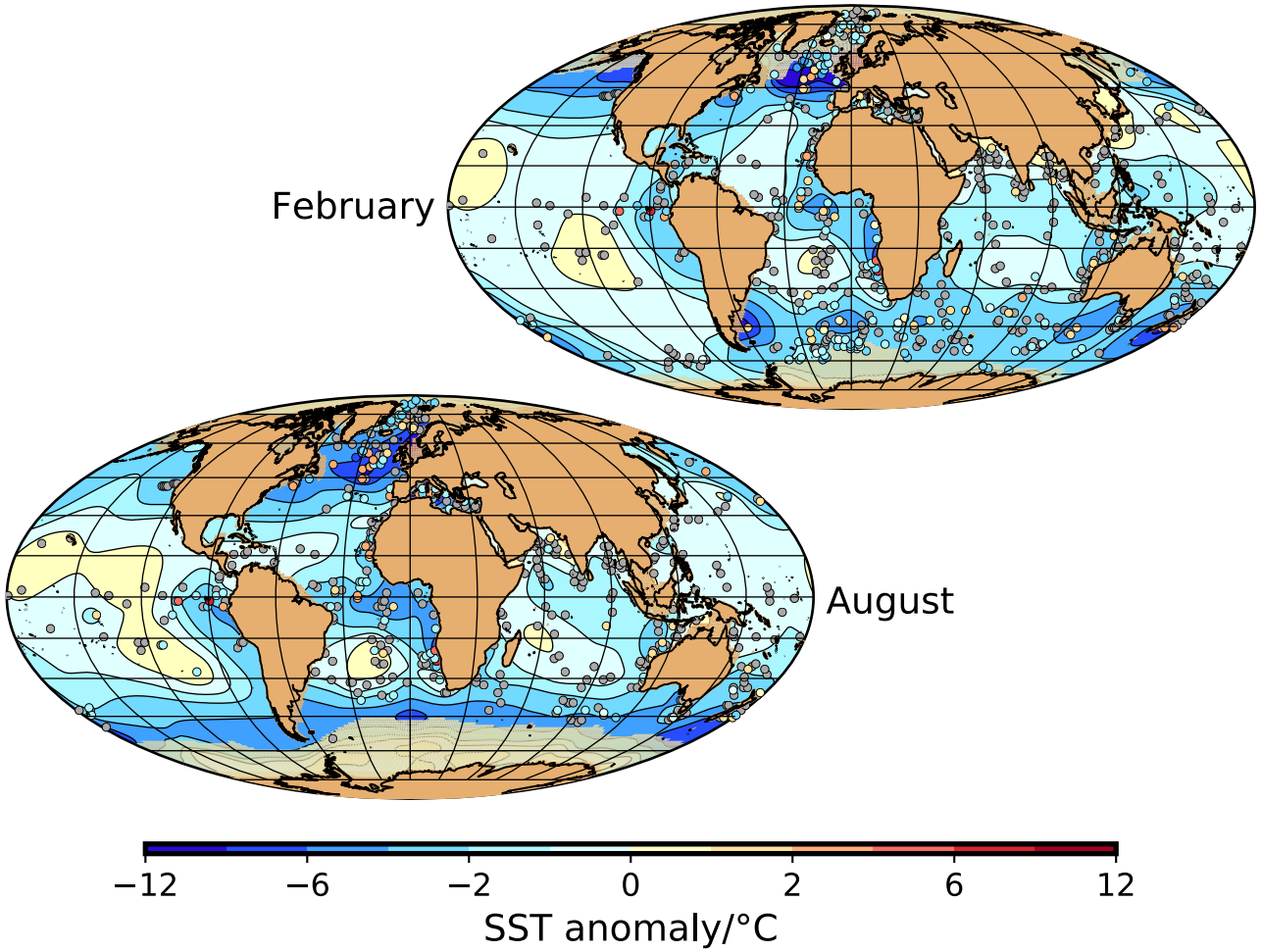

Figure 5. Analyzed SST anomalies for February and August (contour map) and differences between the gridded values and the block-averaged original data values (colored circles – differences smaller than the uncertainty of the data are shown in dark grey.).

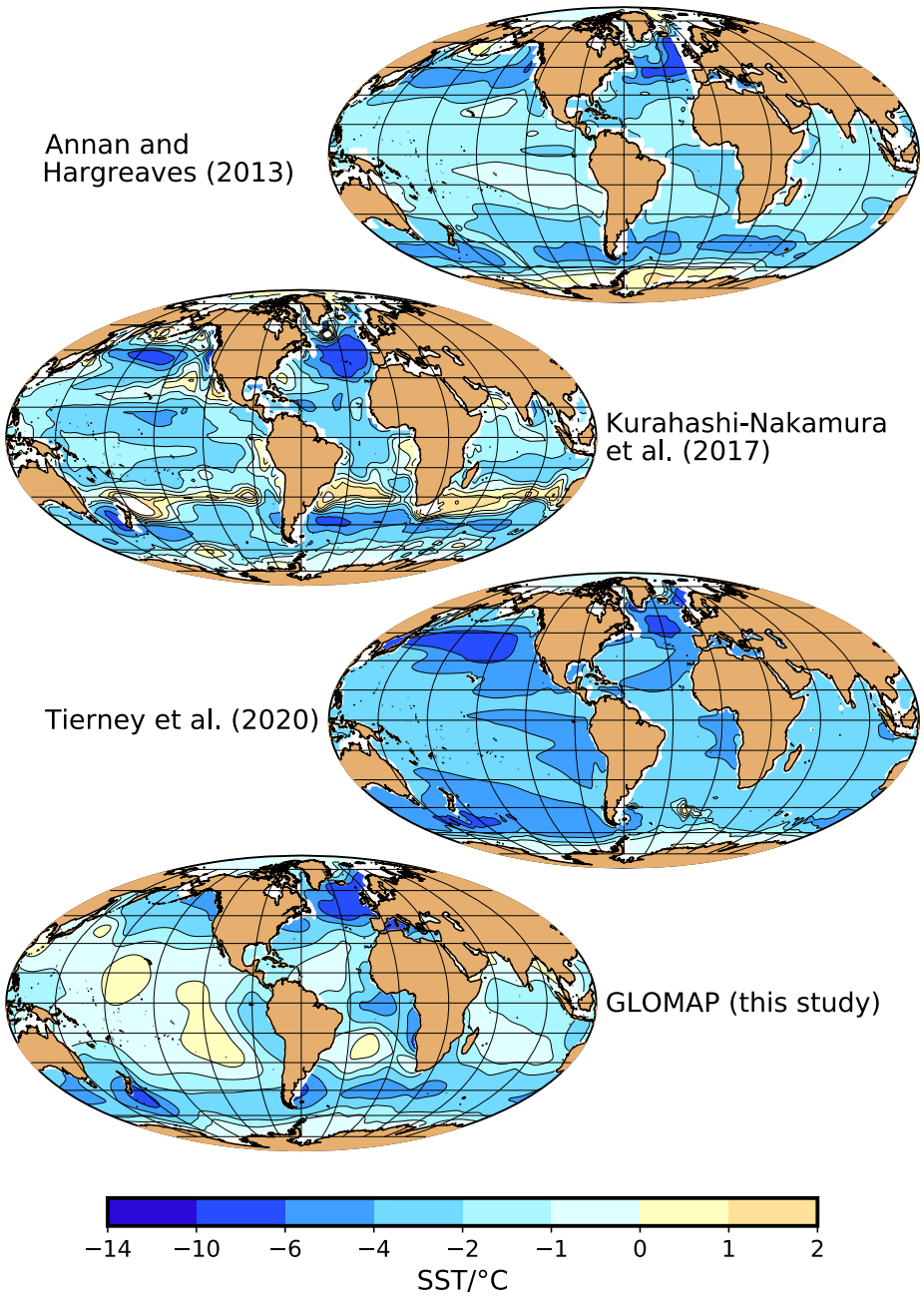

Figure 6. Annual-mean sea-surface temperature anomalies for the LGM according to the reconstructions by Annan and Hargreaves (2013), Kurahashi-Nakamura et al. (2017b) and Tierney et al. (2020) on the one hand and GLOMAP on the other hand.

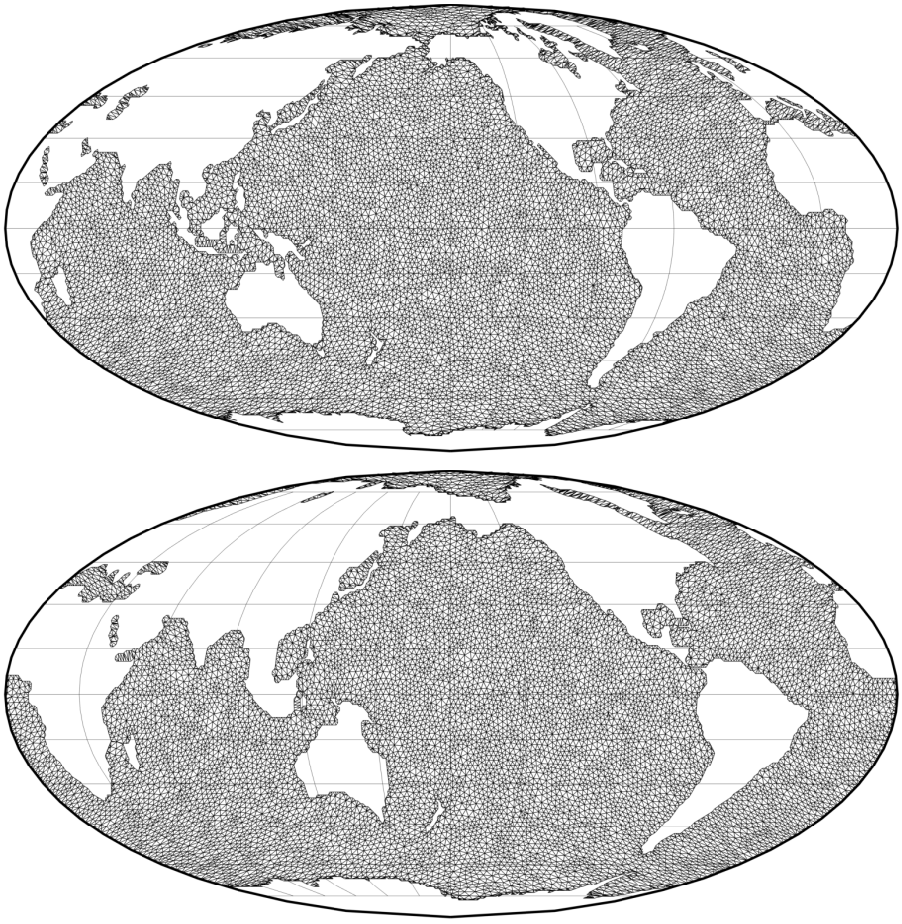

Figure A1. Coastline contours and finite-element meshes for "'original grids"'. Top: for the WOA test of the DIVA method (centered on 210° W). Bottom: for the GLOMAP analysis (centered on 180° W)

Appendix A: Maps of coastlines and finite-element meshes, monthly SST anomalies and their estimated uncertainties

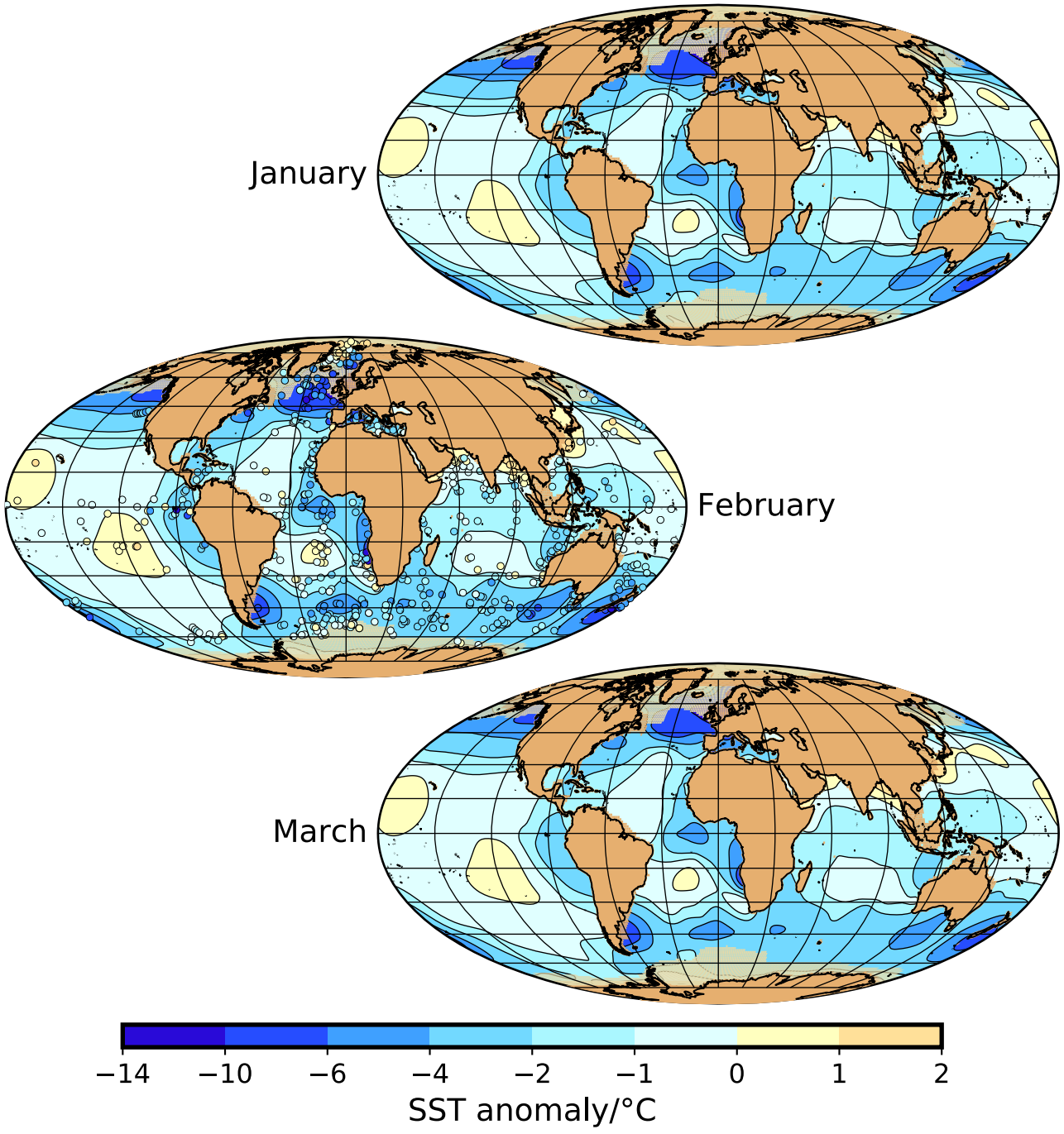

Figure A2. Sea-surface temperature anomaly and sea-ice extent for January, February and March. For February, we also show the MARGO reconstruction at the sediment core locations.

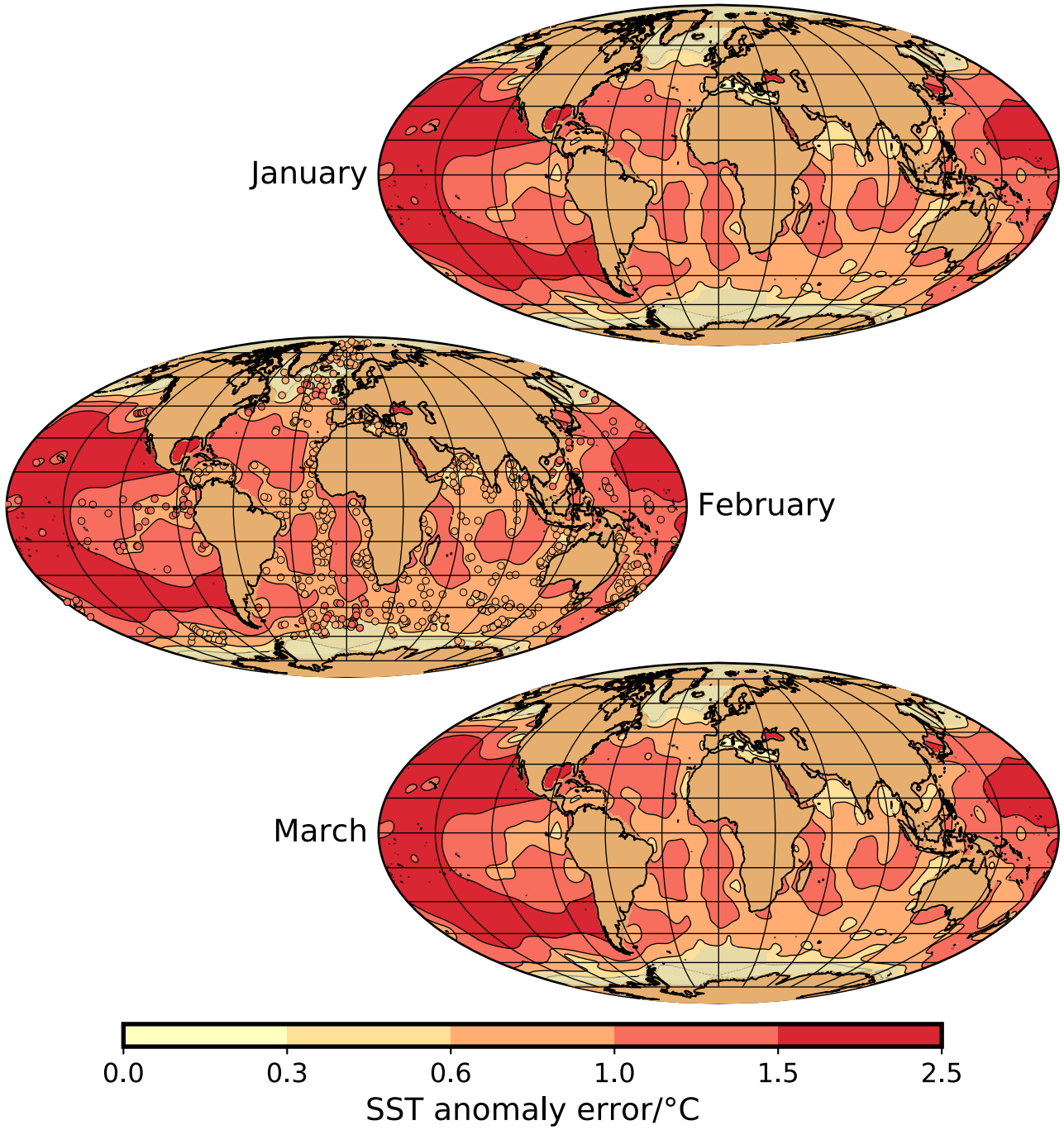

Figure A3. Uncertainty of SST anomaly for January, February and March. For February, we also show the estimated error of the MARGO reconstruction at the sediment core locations.

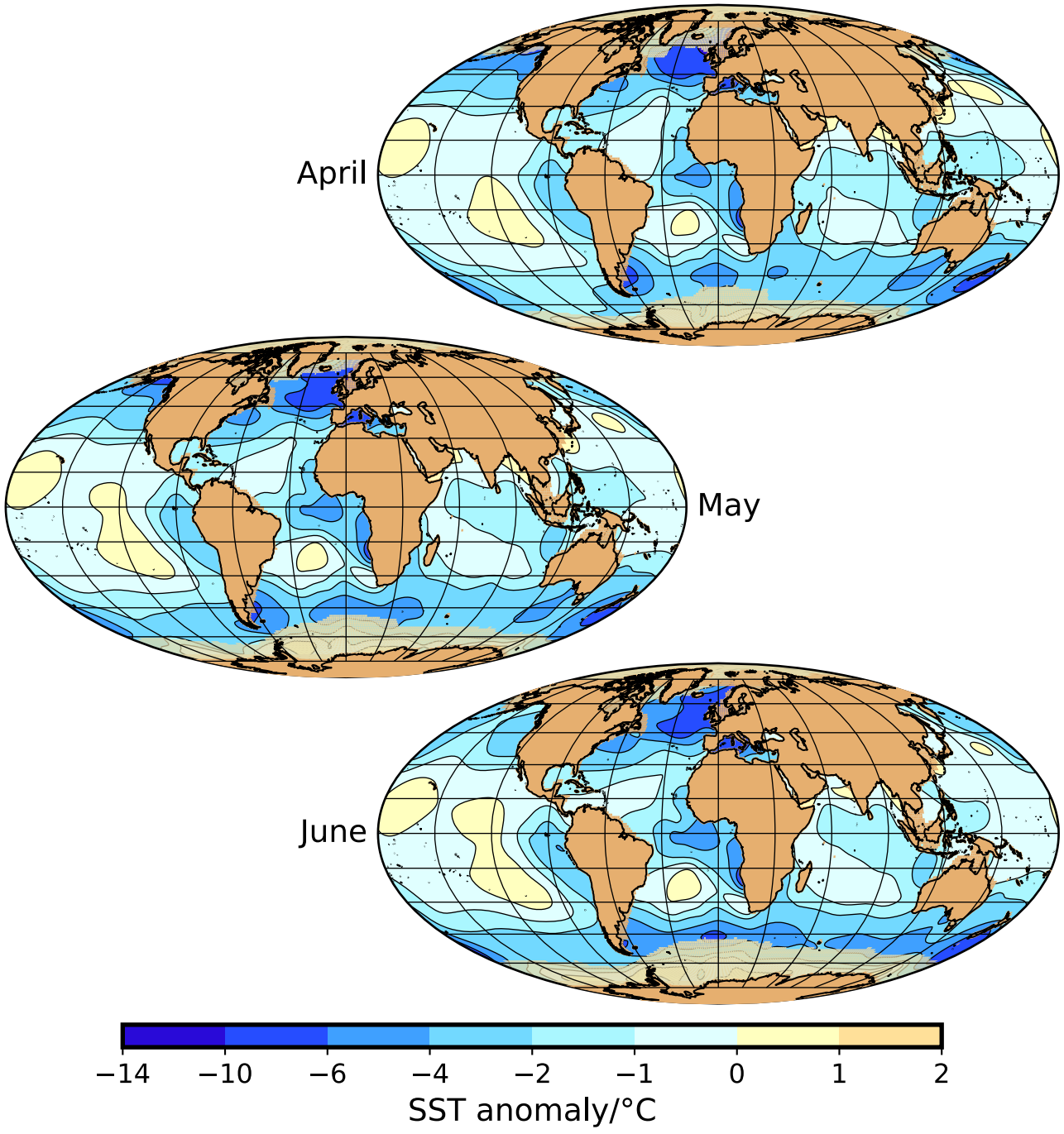

Figure A4. Sea-surface temperature anomaly and sea-ice extent for April, May and June

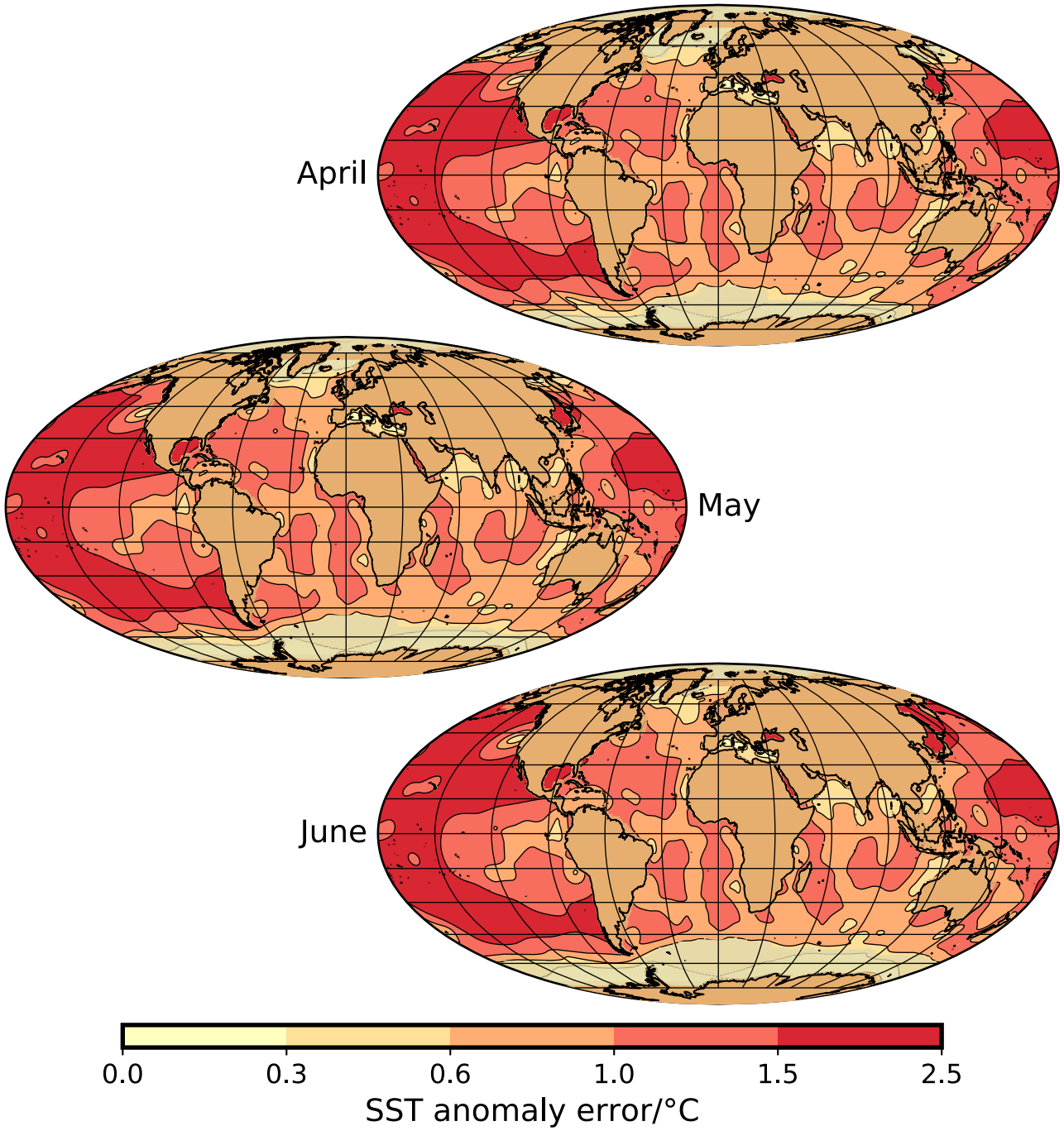

Figure A5. Uncertainty of SST anomaly for April, May and June

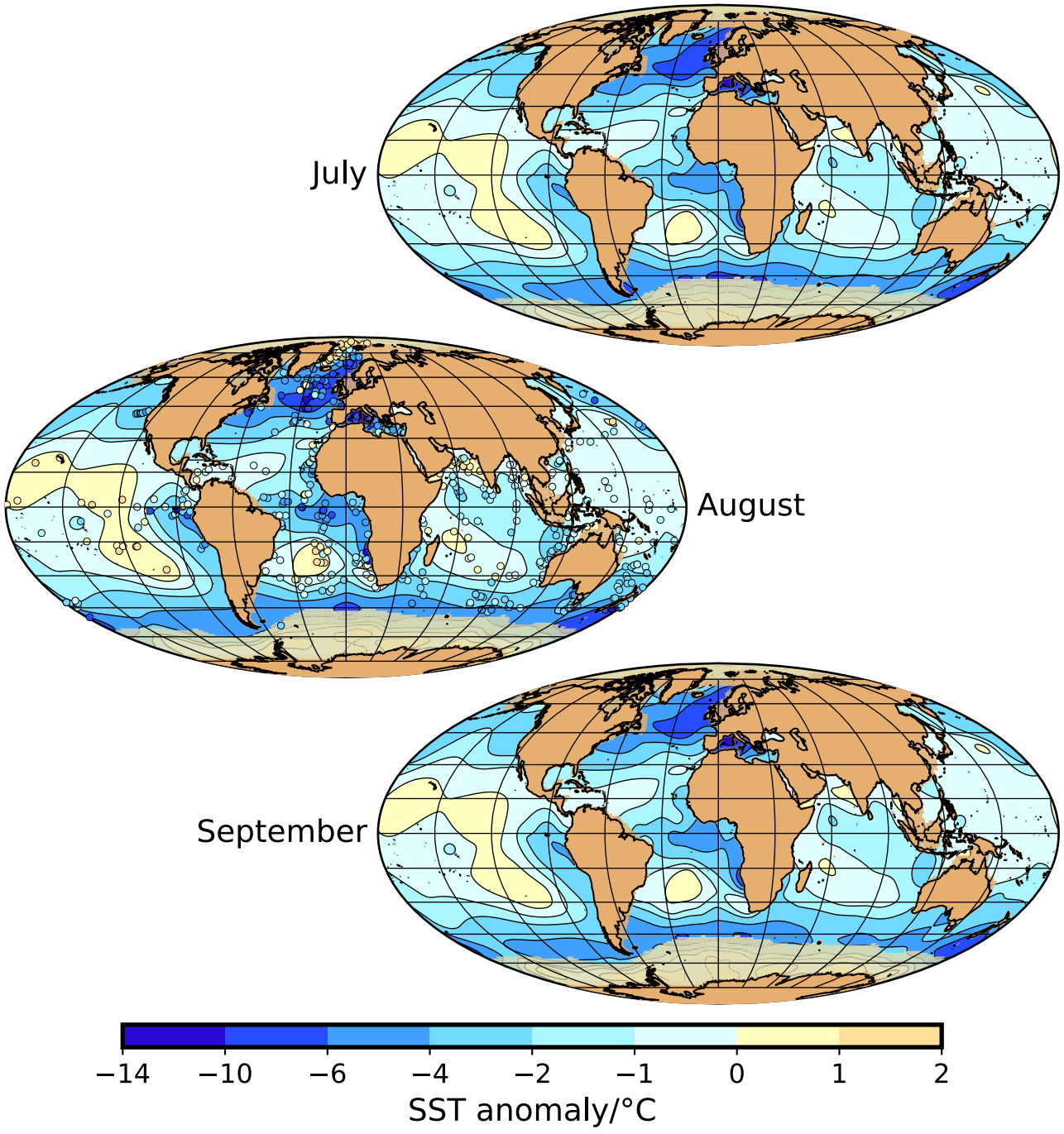

Figure A6. Sea-surface temperature anomaly and sea-ice extent for July, August and September. For August, we also show the MARGO reconstruction at the sediment core locations.

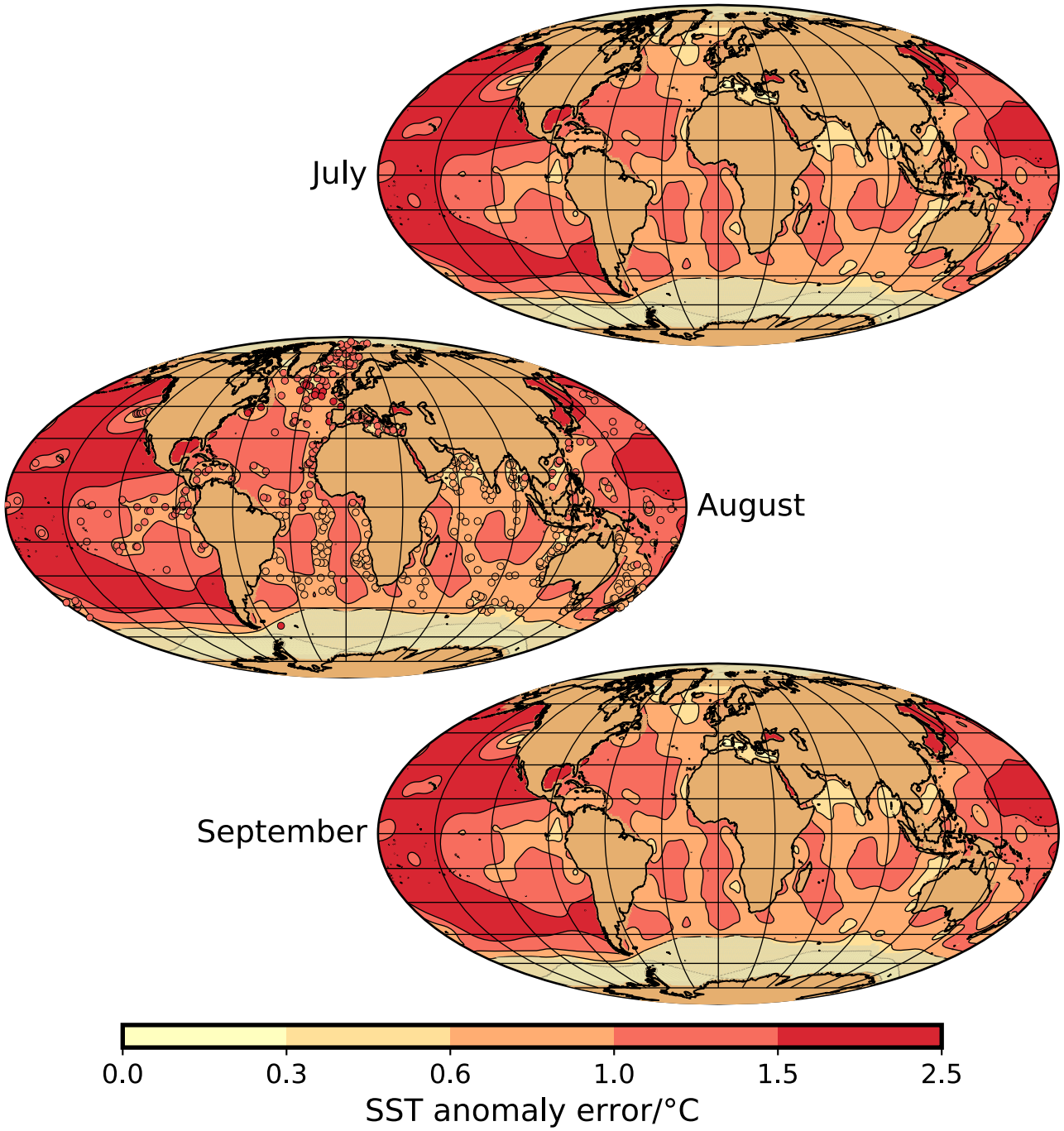

Figure A7. Uncertainty of SST anomaly for July, August and September. For August, we also show the estimated error of the MARGO reconstruction at the sediment core locations.

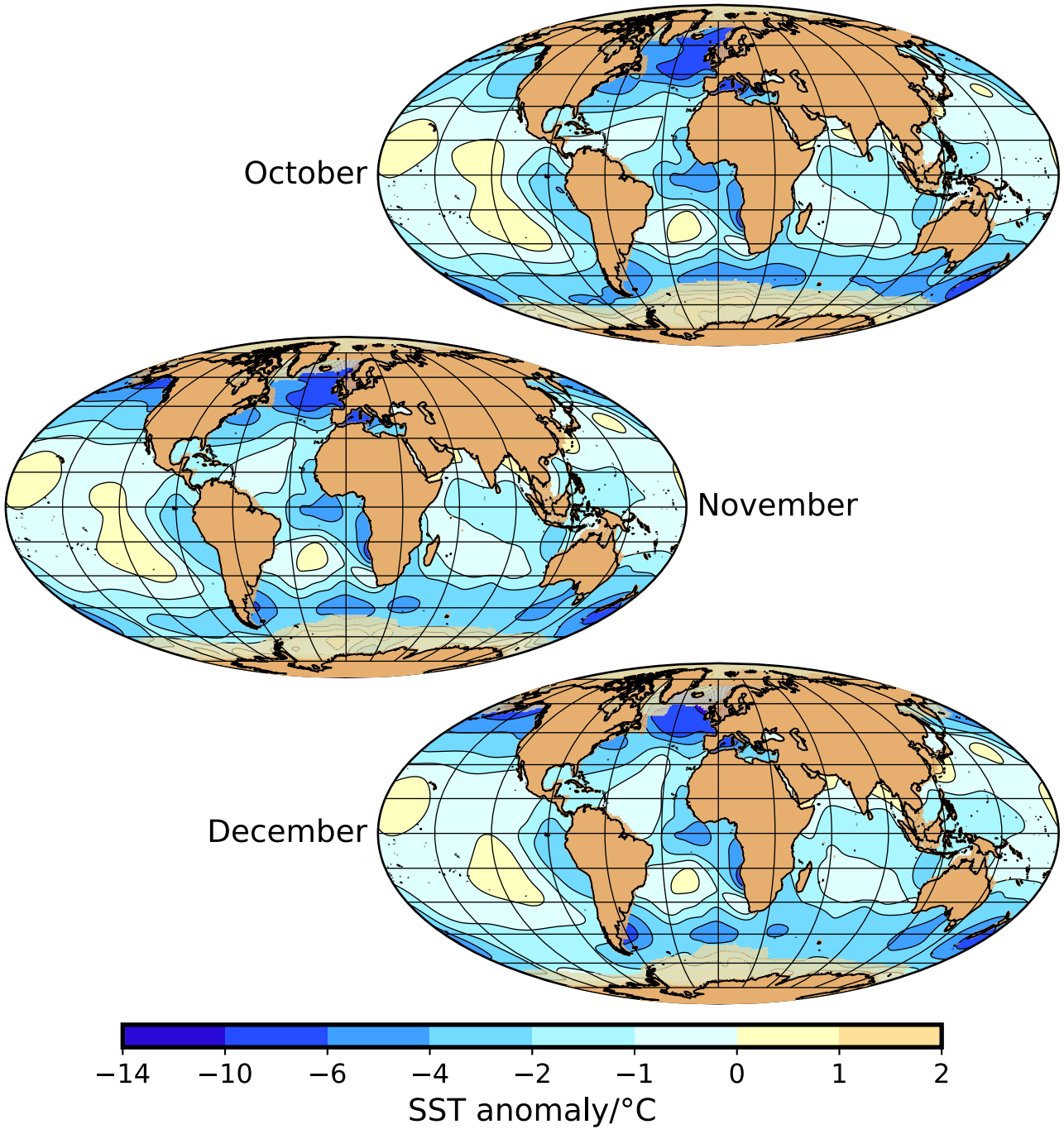

Figure A8. Sea-surface temperature anomaly and sea-ice extent for October, November and December

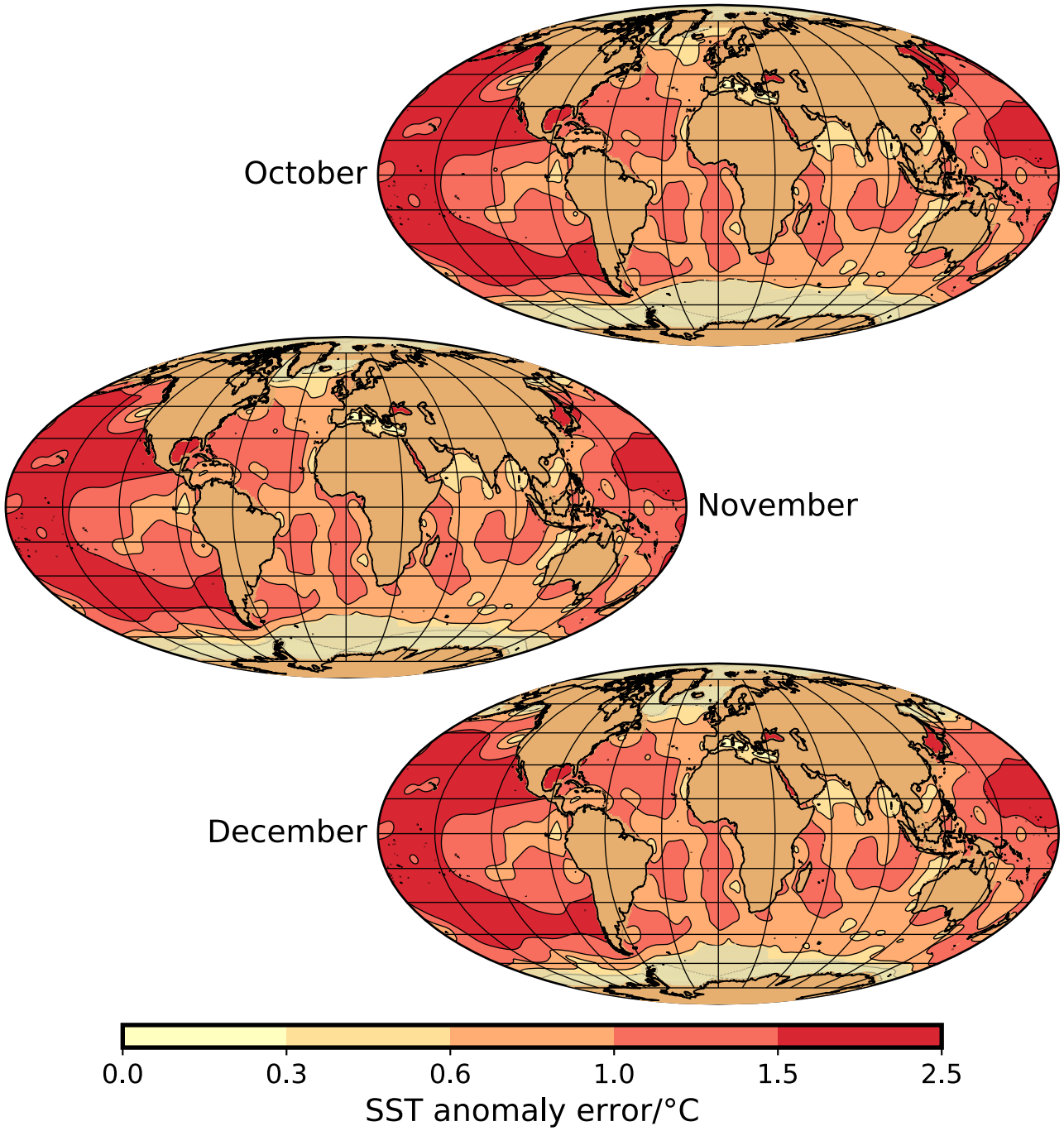

Figure A9. Uncertainty of SST anomaly for October, November and December